Transfer Processes in Turbulent Pipe Flow Described by the ERSR Model

Jan M. H. Fortuin, Edward E. Musschenga, and Peter J. Hamersma
Dept. of Chemical Engineering, University of Amsterdam, 1018 WV Amsterdam, The Netherlands

A model is presented for a quantitative prediction of the transfer rates of momentum, heat and mass in turbulent pipe flow. In this so-called extended random surface renewal (ERSR) model, the tube wall is assumed to be covered by a mosaic of fluid elements of random age and laminar flow with unsteady profiles of axial velocity, temperature or concentration.

Both the age distribution and the mean age of the fluid elements at the tube wall, predicted by the ERSR model, quantitatively agree with experimental results obtained from velocity signals measured with a laser-Doppler anemometer at $5 \cdot 10^3 \leq Re \leq 43 \cdot 10^3$. *The time-averaged radial profiles of the axial velocity, the temperature and the concentration in the wall region, and the heat- and mass-transfer coefficients derived with the ERSR model agree with empirical results presented in literature. Furthermore, the ERSR model provides a basis for explaining the Chilton-Colburn analogy.*

Introduction

Scope

Accurate prediction of the exchange of momentum, heat and mass between a turbulent fluid flow and an interface is often required for equipment design in industry. Most industrial processes, depending on mass transfer, involve one or more fluids in turbulent flow, and the existing theory of turbulence is quite inadequate as a basis for the development of a practically useful theory of mass transfer at a phase boundary. This lack of understanding of turbulence presents a major stumbling block to the development of a theoretical basis for mass transfer between phases (Sherwood et al., 1975).

The need for a reliable model for calculating transfer coefficients in turbulent fluid flow can be elucidated best by the following quote of Batchelor (1957), a well-known authority on fluid mechanics: "Modern technology needs help in describing and analyzing turbulent flows, and cannot wait for scientists to understand its mysteries. Some kind of rational analysis of turbulence is demanded, in such a form that an engineer can apply it with understanding and confidence in many different situations." Written in 1957 this is evidently still true. Of necessity, therefore, the existing correlations of data on transport rates are largely empirical. These have proved extremely useful in the design of process equipment, although the needed data and correlations are often missing or provide only approximate estimates of the size of the mass-transfer devices and of their performance. Nevertheless, the design engineer must use the tools available within the constraints of both equilibrium limitations and economics.

In this article, a *practically useful model*, based on defensible assumptions, will be presented concerning momentum, heat, and mass transfer in turbulent pipe flow. This model cannot completely unlock the above-mentioned "mysteries of turbulence," but the authors hope that it may contribute to the understanding of the mechanisms of momentum, heat and mass transfer between a turbulent fluid flow and a tube wall.

Surface-renewal concept

In turbulent bounded shear flows, the major part of the resistance to the exchange of heat or mass between the bulk of the fluid and the interface is often confined to the so-called "viscous sublayer." The classical theories consider the sublayer motion as a steady mean flow upon which small turbulent fluctuations are imposed. However, hydrodynamic studies of many investigators such as Kline et al. (1967), Corino and

Correspondence concerning this article should be addressed to J. M. H. Fortuin.

Brodkey (1969), and Kim et al. (1971) indicate the existence of motions of well-ordered *fluid elements*, suggesting that the wall region in a turbulent fluid flow consists of a mosaic of *laminar flowing* fluid elements which are *renewed randomly*.

Many authors, working in the field of chemical engineering, civil engineering, and mechanical engineering, have developed *surface-renewal* models to predict the transfer rates of momentum, heat and mass between a turbulent flowing fluid and an interface. In 1935, Higbie pointed out that industrial contactors often operate with repeated brief contacts between phases in which the contact times are too short for the steady state to be achieved. Higbie advanced a theory that in a *packed tower* used for gas absorption, for example, the liquid flows across each packing piece in laminar flow and is remixed at the positions of discontinuity between the packing elements. At such a position, a fresh liquid surface is formed which, as it moves along the packing element, absorbs gas at a decreasing rate until it is mixed at the next discontinuity. Because the liquid flow near the *gas-liquid* interface is only weakly shear-bounded, plug flow approximately occurs and the mass transfer may be considered as a semi-infinite diffusion of mass into a stagnant liquid during its residence time on a packing element. Further, Higbie assumed that in this case all liquid elements have *equal* contact times or *equal* ages.

In *turbulent* flowing liquids, Danckwerts (1951) introduced the *random* surface-renewal concept to describe the mechanism of *gas absorption*, where mass transfer occurs from the gas-liquid interface to the bulk of the liquid. The basis of this random surface-renewal concept is that liquid elements at the *gas-liquid* interface are exchanged randomly in time with elements from the bulk of the turbulent liquid. For the relatively short residence times of these liquid elements at the gas-liquid interface, the elements are assumed to be *stagnant* or *plug flowing*, and the transfer of mass is calculated using the penetration theory.

Other authors have applied the surface-renewal concept to *turbulent shear flows*, such as the *growth-breakdown* models or *periodic-viscous-sublayer* models of Einstein and Li (1956), Ruckenstein (1958), Nijsing (1969), Meek and Baer (1970), and Pinczewski and Sideman (1974), the *film-penetration* model of Toor and Marchello (1958), the *random-surface-renewal* models of Hanratty (1956), Thomas (1978), Klijn (1979), and Fortuin and Klijn (1982), the *surface-rejuvenation* models of Harriot (1962), Thomas (1975, 1980), and Loughlin et al. (1985), or the *random-growth-breakdown* model of Hart (1988). A compilation of various surface-renewal models was published by Sideman and Pinczewski (1975) and Brodkey et al. (1978).

In *turbulent pipe flow*, for example, each fluid element at the *fluid-solid* interface is shear-bounded, which results in a *laminar* flow in the fluid elements with a time-dependent velocity gradient at the fluid-solid interface. If this velocity gradient is not taken into account and the fluid elements are assumed to be stagnant, or plug flowing, the surface-renewal theory applied to turbulent pipe flow, predicts that the Sherwood (or Nusselt) number is proportional to the square root of the Schmidt (or Prandtl) number. However, it is found experimentally that the Sherwood (or Nusselt) number is proportional to the 1/3 power of the Schmidt (or Prandtl) number for values of the Schmidt (or Prandtl) number larger than one. In the present work, it will be shown that a suitable model for the description of the transfer processes in turbulent pipe flow for values of the Schmidt (or Prandtl) number larger than one can be obtained if both a *random age* and a *laminar flow* with a *time-dependent velocity gradient* at the fluid-solid interface are ascribed to the fluid elements at the tube wall.

Klijn (1979) and Fortuin and Klijn (1982) were the first who developed a model, called the RSR model, for turbulent pipe flow to describe the momentum transfer from fluid elements of *laminar flow* and *random age* to the tube wall. This approach resulted in a relationship between the mean age t_0 of the fluid elements at the tube wall, the friction factor f, and the Reynolds number Re. The random distribution of the ages of the fluid elements at the tube wall has been derived from velocity signals measured with a laser-Doppler anemometer by Van Maanen and Fortuin (1982, 1983). A quantitative agreement between measured and calculated values of t_0 has been obtained by Musschenga et al. (1990).

A survey of some of the above-mentioned surface renewal models is given in Table 1. In this table, each type of the surface-renewal models mentioned is characterized by three assumptions that refer to the age, the flow regime, and the approach distance to the wall of the fluid element considered.

In this article, the RSR model of Fortuin and Klijn (1982) is extended to describe heat- and mass-transfer processes in turbulent pipe flow assuming that the tube wall is covered by a mosaic of fluid elements of *laminar* flow and *random* age. This so-called extended random surface renewal (ERSR) model for turbulent pipe flow will be used:

- To derive a relationship between the friction factor and the mean value of the randomly distributed ages of the fluid elements at the tube wall; it will be shown that the *age distribution* and the *mean age* of the fluid elements at the tube wall agree quantitatively with experimental results obtained from velocity signals measured with a laser-Doppler anemometer in turbulent pipe flow.
- To calculate the time-averaged radial profiles of the axial velocity, the temperature and the concentration in the wall region.
- To derive equations for a quantitative prediction of heat- and mass-transfer coefficients.
- To provide a basis for explaining the analogy between momentum, heat, and mass transfer in turbulent pipe flow.

ERSR Model

Introduction

Modeling of transfer processes in turbulent pipe flow should preferably be based on the *observed behavior* of the fluid in the wall region. Hydrodynamic studies have shown that a fluid in turbulent motion may be considered as a mass of fluid elements of indefinite shape and size, which continually change their conformation and position. The fluid elements intermittently move from the bulk of the turbulent fluid toward the interface where they replace other fluid elements. In turbulent pipe flow, the phenomenon of the inrush and ejection of a fluid element at the tube wall is called a *surface renewal*. The fluid elements are assumed to maintain their identity during their residence time at the fluid-solid interface, while momentum and heat or mass are exchanged simultaneously between the fluid elements and the interface. The *average time interval* between two successive surface renewals, which is much greater

Table 1. Survey of Surface-Renewal Models

References	Type		Fluid Elements with				
	Transfer	Interface	Equal Age	Random Age	Plug Flow	Laminar Flow	Approach Distance
Higbie (1935)	mass	*G/L*	×		×		$y=0$
Danckwerts (1951)	mass	*G/L*		×	×		$y=0$
Einstein & Li (1956)	momentum	*F/S*	×			×	$y=0$
Hanratty (1956)	momentum	*F/S*	×			×	$y=0$
	heat		×	×	×		
	mass		×	×	×		
Harriott (1962)	mass	*F/S*		×	×		$y=R$
Pinczewski & Sideman (1974)	heat	*F/S*	×			×	$y=0$ or constant
	mass		×			×	
Thomas (1980)	momentum	*F/S*		×		×	$y=R$
	heat			×	×		
Fortuin & Klijn (1982)	momentum	*F/S*		×		×	$y=0$
Loughlin et. al. (1985)	momentum	*F/S*		×		×	$y=R$
	heat			×	×		
	mass			×	×		
Hart (1988)	momentum	*F/S*		×		×	$y=0$
	heat			×		×	
	mass			×		×	
present paper	momentum	*F/S*		×		×	$y=0$
	heat			×	×	×	
	mass			×	×	×	

F = fluid *L* = liquid *S* = solid *G* = gas *R* = random

the short time required for the renewal process itself, is considered as the *age* of the *laminarly* flowing fluid element at the tube wall.

For the mathematical formulation of the transfer mechanisms, it is unimportant whether the renewal of the laminar flowing fluid element at the interface is caused by the inrushing high-momentum fluid elements or, as suggested by Einstein and Li (1956), by the spontaneous breakdown of the viscous sublayer due to instabilities (Sideman and Pinczewski, 1975, p. 168.)

Assumptions

The ERSR model is developed for the description of momentum, heat and mass transfer occurring at the wall of a fully developed turbulent flow of a single-phase Newtonian fluid in a straight, *smooth* tube. The model is based on the following 12 physically acceptable assumptions:

1. The fluid is incompressible and has constant transport properties (ρ,η,c_p,λ,D, and σ), the values of which are independent of time and position in the fluid.

2. The local time-averaged flux ($0 \le t \le \infty$) at an arbitrary fixed position at the tube wall is equal to the instantaneous flux averaged over the whole surface of the wall.

3. The tube wall is covered by a mosaic of fluid elements of *random age* and *laminar flow* with unsteady radial profiles of axial velocity, temperature or concentration.

4. The local instantaneous flux of momentum, heat or mass at the tube wall ($y=0$) is proportional to the instantaneous local radial gradients of the axial velocity, the temperature or the concentration, respectively.

5. The local time-averaged flux of momentum, heat or mass at the tube wall may be calculated from the radial gradients of the axial velocity, the temperature or the concentration, respectively, at one single position at the wall in the whole time domain.

6. At an arbitrary fixed position at the tube wall, the radial gradients can instantaneously be changed by an inrushing fluid element with bulk-fluid properties, which renews the local near-wall fluid completely.

7. During the time interval between two successive renewals, which is considered as the age of a fluid element at the tube wall, unsteady momentum, heat, or mass transfer takes place.

8. At a given Reynolds number, the chance that during an infinitesimally small time interval a surface renewal occurs at an arbitrary fixed position at the wall is independent of the age or position of the fluid element at the tube wall.

9. The ratio between the average *penetration depth* of momentum, heat or mass and the *radius* of the tube is so small (for example, less than 0.10) that the curvature of the interface may be neglected. Further, the axial velocity in the bulk of the fluid is assumed to be equal to the average value of the fluid velocity over the cross-section of the tube. These assumptions approximately hold for $Re \ge 10^4$ (Fortuin and Klijn, 1982).

10. The average time interval during which a surface re-

newal occurs is negligibly small in comparison with the average time interval between two successive renewals.

11. In liquid elements at a *gas-liquid* interface plug flow occurs, because the fluid elements at such an interface are approximately not shear-bounded.

12. In fluid elements at a *fluid-solid* interface plug flow only occurs, if the penetration depth of the heat or mass is larger than the penetration depth of momentum ($Pr<1$ or $Sc<1$). However, if the penetration depth of heat or mass is small compared with the penetration depth of momentum ($Pr>1$ or $Sc>1$), laminar flow occurs with a velocity gradient at the interface.

Constraints

The ERSR model can be used to describe momentum, heat, and mass transfer in a fully developed turbulent pipe flow at $Re \geq 10^4$ with relatively small rates of heat or mass transfer (for example, during electrolysis at a smooth electrode (Mizushina et al., 1971), and during the onset of fouling and corrosion), excluding chemical reactions in the fluid, density gradients (natural convection), surface-tension gradient (Marangoni effect), drift effects, and viscous dissipation.

Further, the concept of a valid analogy among momentum, heat, and mass transfer is that the basic transfer mechanisms are similar. The analogy between momentum transfer and heat or mass transfer is valid only if there is no form drag. Thus, the analogy cannot be applied to any flow for which separation of the boundary layer occurs (Brodkey and Hershey, 1989). Flow in ducts and over flat plates do qualify, however. The analogy breaks down for rough tubes in fully developed turbulent flow because the friction factor is differently affected by roughness than the heat- or mass-transfer coefficients. Further, it has to be noted that relatively large values of temperature and concentration gradients can lead to transport-property gradients which significantly affect the profiles of the axial velocity, the temperature, and the concentration in the wall region, the transfer rates in the fluid elements at the interface, and probably also the surface-renewal frequency.

Transfer processes at an interface

If $F(y,t)$ denotes a *local instantaneous physical quantity* (for example, the axial velocity u, the temperature T, and the concentration c) in a fluid element at a distance y to the tube wall and after a residence time t at the wall, the *local age-averaged physical quantity* $\bar{F}(y,\theta)$ can be obtained from:

$$\bar{F}(y,\theta) = (1/\theta)\int_0^{\theta} F(y,t)\,dt \tag{1}$$

If the chance that a fluid element at the tube wall has an age between θ and $\theta+d\theta$ is given by $\varphi(\theta)d\theta$, the *local time-averaged physical quantity* $\bar{F}(y)$ follows from:

$$\bar{F}(y) = \frac{\int_0^{\infty} \theta \left\{(1/\theta)\int_0^{\theta} F(y,t)\,dt\right\}\varphi(\theta)\,d\theta}{\int_0^{\infty} \theta\varphi(\theta)\,d\theta} \tag{2}$$

If during an infinitesimally small time interval the chance that a fluid element is renewed is constant, that is, independent of its age or position at the tube wall, the *age distribution* follows from (Danckwerts, 1951; Klijn, 1979; Fortuin and Klijn, 1982):

$$\varphi(\theta)d\theta = e^{-\theta/t_0}d(\theta/t_0) \tag{3}$$

In Eq. 3, t_0 represents a *characteristic value of the ages* of the fluid elements at the tube wall; this value depends on the flow conditions ($\langle u\rangle$, ν, ρ, and d), and will be expressed in Eq. 19. It may be noted that the random-age distribution is not applied for the sake of mathematical convenience and simplicity, but because Eq. 3 has been verified experimentally, as will be discussed later.

Referring to Eq. 3, the *mean age* of the fluid elements at the interface follows from:

$$\bar{\theta} = \int_0^{\infty} \theta\varphi(\theta)\,d\theta = t_0 \tag{4}$$

The reciprocal value of the mean age t_0 is defined as the *characteristic renewal frequency* n_0.

Combination of Eqs. 2, 3 and 4 results in:

$$\bar{F}(y) = (1/t_0)\int_{\theta=\infty}^{\theta=0} \left\{\int_0^{\theta} F(y,t)\,dt\right\} d(e^{-\theta/t_0}) \tag{5}$$

Partial integration of Eq. 5 leads to:

$$\bar{F}(y) = \int_0^{\infty} F(y,\theta)e^{-\theta/t_0}d(\theta/t_0) \tag{6}$$

The value of $\bar{F}(y)$ does not change if θ is replaced by t, so that the *local time-averaged physical quantity* can be obtained from:

$$\bar{F}(y) = \int_0^{\infty} F(y,t)e^{-t/t_0}d(t/t_0) \tag{7}$$

Note that if $1/t_0 = s$, the time-averaged physical quantity $\bar{F}(y)$ can be obtained from Eq. 7 by calculating the Laplace transform of $F(y,t)$ *without inversion*, divided by t_0:

$$\bar{F}(y) = (1/t_0)L\{F(y,t)\} \tag{8}$$

If the *local time-averaged flux* $\bar{J}_w$ (the local momentum, heat, or mass flux) at the tube wall is the product of a *transport property* β (η, λ, or D) and the gradient $\{\partial\bar{F}(y)/\partial y\}_{y=0}$ of the local time-averaged physical quantity $\bar{F}(y)$, the flux $\bar{J}_w$ can be obtained from:

$$\bar{J}_w = \beta\{\partial\bar{F}(y)/\partial y\}_{y=0} \tag{9}$$

Combining Eqs. 7 and 9 results in:

$$\bar{J}_w = \beta\frac{\partial}{\partial y}\left(\int_0^{\infty} F(y,t)e^{-t/t_0}d(t/t_0)\right)_{y=0} \tag{10}$$

or

$$\bar{J}_w = \int_0^\infty J_w(t) e^{-t/t_0} d(t/t_0), \text{ where } J_w(t) = \beta \left(\frac{\partial F(y,t)}{\partial y} \right)_{y=0} \tag{11}$$

In this section, it has been shown, that if the *local instantaneous* physical quantity $F(y,t)$ is known, both the local *time-averaged* physical quantity $\bar{F}(y)$ and the corresponding *flux* $\bar{J}_w$ at the tube wall can be calculated from Eqs. 7 and 11, respectively. In the following sections, equations will be derived for the local instantaneous and the time-averaged values of the momentum, heat and mass fluxes at the tube wall, and the local instantaneous and time-averaged values of the axial velocity, the temperature and the concentration in the wall region.

Momentum Transfer

Time-averaged wall-shear stress

Upon its arrival at the wall, an inrushing fluid element gradually loses momentum as a result of viscous interaction with the wall. In this fluid element, which originally traveled with a uniform velocity approximately equal to the average velocity of the fluid in the turbulent core, a velocity profile starts to develop. The development of this velocity profile and the average transfer rate of momentum to the wall can approximately be described by a reduced equation of motion:

$$\partial u/\partial t = \nu \partial^2 u/\partial y^2 \tag{12}$$

This equation for the unsteady transfer of momentum from a laminar flowing fluid element to the pipe wall can be solved using the initial condition (IC) and the boundary condition (BC):

$$\begin{aligned} &IC: \quad t=0;\ y \geq 0;\ u = u_b, \\ &BC: \quad t>0;\ y=0;\ u=0, \\ &BC: \quad t>0;\ y=\infty;\ u=u_b. \end{aligned} \tag{13}$$

The solution to Eq. 12 with the conditions of Eq. 13 is:

$$u(y,t)/u_b = \text{erf}(z), \text{ where } z = \frac{y}{2\sqrt{(\nu t)}} \tag{14}$$

The *local instantaneous shear stress* $\tau_w(t)$ exerted on the wall by a single laminar flowing fluid element is obtained from:

$$\tau_w(t) = \eta \left(\frac{\partial u}{\partial y} \right)_{y=0} = \nu \rho u_b (\pi \nu t)^{-1/2} \tag{15}$$

The *local time-averaged stress* $\bar{\tau}_w$ at the tube wall can be derived from Eqs. 11 and 15 by substituting $\tau_w(t)$ for $J_w(t)$:

$$\bar{\tau}_w = \nu \rho u_b (\nu t_0)^{-1/2} \tag{16}$$

Combining Eq. 16 with $u_b \approx \langle u \rangle$ and the definition of the Fanning friction factor:

$$f = \bar{\tau}_w \Big/ \left(\frac{1}{2} \rho \langle u \rangle^2 \right) \tag{17}$$

results in the following equation:

$$f = 2 \left(\frac{d}{\sqrt{(\nu t_0)}} \right) \left(\frac{\nu}{\langle u \rangle d} \right) = 2 Fo^{-1/2} Re^{-1} \tag{18}$$

Equation 18, first introduced by Fortuin and Klijn (1982), gives the relationship between the *friction factor* in turbulent pipe flow and the *mean age* of the fluid elements at the tube wall. Rewriting Eq. 18, and using $t_0 = 1/n_0$ result in:

$$t_0 = (1/n_0) = \left(\frac{1}{2} f \cdot Re \right)^{-2} d^2/\nu \tag{19}$$

It has to be noted that n_0 is the reciprocal value of the mean age, *not* the mean value of the renewal frequency (Fortuin and Klijn, 1982).

It will be shown later that the age distribution calculated with Eq. 3 of the ERSR model, and the values of t_0 calculated with Eq. 19 agree quantitatively with the age distribution and values of $\bar{\theta}_{exp}$ obtained from velocity signals measured with a laser-Doppler anemometer.

Time-averaged axial velocity profile in the wall region

The *local time-averaged axial velocity* $\bar{u}(y)$ in the wall region is obtained by substituting $u(y,t)$ of Eq. 14 for $F(y,t)$ into Eq. 7:

$$\bar{u}(y) = \int_0^\infty u(y,t) e^{-t/t_0} d(t/t_0) \tag{20}$$

Defining

$$z_0 = \frac{y}{2\sqrt{(\nu t_0)}} \tag{21}$$

Equation 20 results in:

$$\bar{u}(y)/u_b = 1 - \frac{2}{\sqrt{\pi}} \int_0^\infty e^{-(z^2 + z_0^2/z^2)} dz \tag{22}$$

After substitution of the solution to the definite integral (Weast, 1972) into Eq. 22, the following *axial velocity profile in the wall region* of a turbulent pipe flow is obtained (Klijn, 1979):

$$\bar{u}(y)/u_b = 1 - e^{-2z_0} = 1 - e^{-y/\sqrt{(\nu t_0)}} \tag{23}$$

Using Eq. 19 and $u_b \approx \langle u \rangle$, the time-averaged axial velocity profile in the wall region can be calculated with:

$$\bar{u}(y)/u_b = 1 - e^{-y/\sqrt{(\nu t_0)}} = 1 - \exp\left(-\frac{y}{d} \cdot \frac{f}{2} Re \right) \tag{24}$$

For the calculation of this *general velocity profile* in the wall region given by Eq. 24, only the value of the *friction factor* is needed. In most correlations for the *universal velocity profile* in the wall region in a turbulent pipe flow, two additional empirical constants have to be specified.

An empirical correlation giving sufficiently accurate values for the friction factor for Newtonian fluid flow through straight, smooth tubes in the range $2{,}100 \le Re \le 10^8$ is (Eck, 1973):

$$f = 0.07725/(\log(Re/7))^2 \tag{25}$$

Other well-known correlations between f and Re were proposed by Blasius (1913), Nikuradse (1932), and McAdams (1954).

Equation 24 can be rewritten in the commonly used u^+ against y^+ notation. With $u_b \approx \langle u \rangle$ and defining the following dimensionless quantities $u^* = \sqrt{(\bar{\tau}_w/\rho)}$, $u^+ = \bar{u}(y)/u^*$, $\langle u \rangle^+ = \langle u \rangle / u^*$, and $y^+ = y u^*/\nu$, it can be shown that:

$$u^+/\langle u \rangle^+ = 1 - e^{-y^+/\langle u \rangle^+} \tag{26}$$

Using Eq. 17 it can be obtained that:

$$\langle u \rangle^+ = \langle u \rangle / u^* = \sqrt{(2/f)} \tag{27}$$

The velocity profile in the wall region of a turbulent pipe flow represented in the u^+ against y^+ notation follows from Eqs. 26 and 27:

$$u^+ = (1 - e^{-y^+\sqrt{(f/2)}})/\sqrt{(f/2)} \tag{28}$$

It has to be noted that Thomas (1978) also published a way to derive Eq. 28.

Heat Transfer

In turbulent pipe flow, the heat-transfer process between the tube wall and the turbulent fluid can be described in a similar way as it has been done in the previous section for the local time-averaged wall-shear stress and the time-averaged axial velocity profile in the wall region. In the following, it will be assumed that the tube wall has locally a constant temperature T_w, and that the bulk of the fluid has locally a constant temperature T_b, where $T_w > T_b$. When a fluid element with a uniform velocity u_b and a temperature T_b comes from the turbulent core and arrives at the wall, both momentum and heat are exchanged by diffusion between the interface and the *laminar* flowing fluid element. After a certain residence time θ, the laminar flowing fluid element is replaced suddenly by a new fluid element from the turbulent core, and again momentum and heat are exchanged by diffusion between the new laminar flowing fluid element and the interface. This heat-transfer process may be reduced to a problem of heat transfer into a laminar fluid flow. Solution of the *unsteady* convective-diffusion equation, however, requires numerical computation, which is beyond the scope of this study. Here, we shall restrict ourselves to a model based on simplified, but physically acceptable, assumptions to facilitate analytical solutions.

Time-averaged heat flux through the interface for $Pr > 1$

The heat flux from the tube wall into a laminar flowing fluid element encounters an approximately *linear* velocity profile, if the penetration depth of heat is small with regard to that of momentum ($Pr > 1$). Upon its arrival at the wall, the fluid element gradually decelerates and the velocity of the laminar flow near the interface becomes smaller. The velocity profile in this laminar flowing fluid element can be obtained from Eq. 14 (Abramowitz and Stegun, 1970):

$$u(y,t)/u_b = \mathrm{erf}(z) = \frac{2}{\sqrt{\pi}}\,(z - (z^3/3) + (z^5/10) - \ldots) \tag{29}$$

For small values of z the relative velocity may be approximated by:

$$u(y,t)/u_b \approx \left(\frac{2z}{\sqrt{\pi}}\right) = \left(\frac{y}{\sqrt{(\pi \nu t)}}\right) \tag{30}$$

After its arrival at the wall the instantaneous axial velocity profile in the fluid element is assumed to be *independent* of the longitudinal coordinate x. As a consequence, the *velocity* in the fluid element is only a function of the distance y to the wall and the time t passed since the arrival of the fluid element at the wall. In this case, the heat transfer can be described as a semi-infinite diffusion of heat from the interface into a *laminar* flowing fluid element with a transversal *velocity gradient* $(\partial u/\partial y)_{y=0}$, the value of which depends only on the residence time of the fluid element at the wall and does not change in the direction of x. At a given residence time, however, the *temperature gradient* $(\partial T/\partial y)_{y=0}$ changes in the flow direction. This heat-transfer process is considered to be similar to that occurring during heat transfer from a flat wall into a developing laminar fluid flow. The $\partial T/\partial t$ term in the convective-diffusion equation is neglected so that an analytical solution can be obtained. Further, for small heat fluxes and no suction, the y-directed velocity in the laminar flowing fluid element is approximately zero (Ruckenstein, 1958, 1967; Pinczewski and Sideman, 1974). The resulting heat-transfer problem can be described approximately by the following differential equation (see, for example, Bird et al., 1960; Hoogendoorn, 1985):

$$u(y,t)\,\frac{\partial T(y,x)}{\partial x} = a\,\frac{\partial^2 T(y,x)}{\partial y^2} \tag{31}$$

provided that heat conduction of the fluid in the flow direction is small compared with the forced convective transport in this direction, so that liquid metals are excluded. Relating the time t and the distance x to the velocity u_b of that part of the fluid element that has not been decelerated by the viscous interaction with the tube wall (Pinczewski and Sideman, 1974):

$$\frac{\partial T(y,x)}{\partial x} = \frac{\partial T/\partial t}{\partial x/\partial t} \approx \frac{\partial T(y,t)/\partial t}{u_b} \tag{32}$$

allows Eq. 31 to be rewritten in the form:

$$\left(\frac{u(y,t)}{u_b}\right)\frac{\partial T(y,t)}{\partial t} = a\,\frac{\partial^2 T(y,t)}{\partial y^2} \tag{33}$$

The initial and boundary conditions are:

$$\begin{aligned} &IC: \quad t = 0;\ y \ge 0;\ T = T_b, \\ &BC: \quad t > 0;\ y = 0;\ T = T_w, \\ &BC: \quad t > 0;\ y = \infty;\ T = T_b. \end{aligned} \tag{34}$$

With the definition of z in Eq. 14, it can easily be derived that:

$$\frac{\partial T(y,t)}{\partial t} = \left(\frac{-z}{2t}\right) \frac{dT(y,t)}{dz}$$

$$\text{and } \frac{\partial^2 T(y,t)}{\partial y^2} = \left(\frac{1}{4\nu t}\right) \frac{d^2 T(y,t)}{dz^2} \quad (35)$$

Substitution of Eqs. 30 and 35, and $\nu/a = Pr$ into Eq. 33 results in:

$$d^2T(y,t)/dz^2 + \left(\frac{4Pr\, z^2}{\sqrt{\pi}}\right) dT(y,t)/dz = 0 \quad (36)$$

The transformed initial and boundary conditions of Eq. 34 are:

$$BC: \quad z = 0; \; T = T_w, \quad (37)$$
$$BC: \quad z = \infty; \; T = T_b.$$

Integration of Eq. 36 and using the boundary conditions of Eq. 37 lead to the *instantaneous radial temperature profile* in a laminar flowing fluid element at the tube wall:

$$\frac{T_w - T(y,t)}{T_w - T_b} = \frac{1}{\Gamma(4/3)} \int_0^{\zeta} e^{-\xi^3} d\xi \quad (38)$$

where

$$\zeta = \left(\frac{4Pr}{3\sqrt{\pi}}\right)^{1/3} \cdot \left(\frac{y}{2\sqrt{(\nu t)}}\right) \quad (39)$$

The *local instantaneous heat flux* from the interface into a laminar flowing fluid element is obtained from:

$$q_w(t) = -\lambda \left(\frac{\partial T(y,t)}{\partial y}\right)_{y=0} = -\lambda \left(\frac{dT(y,t)}{d\zeta}\right)_{\zeta=0} \cdot \left(\frac{\partial \zeta}{\partial y}\right) \quad (40)$$

Combination of Eqs. 38, 39 and 40 leads to:

$$q_w(t) = C\lambda (T_w - T_b) (\pi \nu t)^{-1/2} Pr^{1/3} \quad (41)$$

where

$$C = \frac{(\pi/6)^{1/3}}{\Gamma(4/3)} = 0.9026 \quad (42)$$

The *local time-averaged heat flux*, averaged over all possible ages of the fluid elements at the tube wall ($0 < \theta < \infty$), can be obtained from Eqs. 11 and 41:

$$\bar{q}_w = C\lambda (T_w - T_b) (\nu t_0)^{-1/2} Pr^{1/3} \quad (43)$$

Defining $\bar{q}_w = \alpha (T_w - T_b)$ and the *dimensionless time-averaged heat-transfer coefficient* or Nusselt number, $Nu = \alpha d/\lambda$, Eq. 43 can be rearranged to:

$$Nu = Cd (\nu t_0)^{-1/2} Pr^{1/3} \quad (44)$$

Combining Eqs. 18 and 44 results in the following equation:

$$Nu = C(f/2) Re\, Pr^{1/3} \quad (Pr > 1) \quad (45)$$

Using the following correlation between f and Re for turbulent pipe flow, given by McAdams (1954):

$$f = 0.046\, Re^{-0.2} \quad (10^4 \le Re \le 2 \cdot 10^5) \quad (46)$$

and combining Eqs. 42, 45 and 46 result in the following equation for the dimensionless time-averaged heat-transfer coefficient:

$$Nu = 0.021\, Re^{0.80} Pr^{1/3} \quad (10^4 \le Re \le 2 \cdot 10^5;\; Pr > 1) \quad (47)$$

Equation 47 agrees within approximately 10% with the following empirical correlation of Colburn (1933):

$$Nu = 0.023\, Re^{0.80} Pr^{1/3}$$
$$(10^4 \le Re \le 2 \cdot 10^5;\; 0.7 \le Pr \le 700) \quad (48)$$

where the physical properties are taken at the film temperature $T_f = (T_w + T_b)/2$ (Perry and Green, 1984).

Time-averaged radial temperature profile in the wall region for Pr > 1

The *time-averaged radial temperature profile* in the wall region can be obtained from Eq. 7 by substituting $T(y,t)$ for $F(y,t)$:

$$T_w - \bar{T}(y) = \int_0^{\infty} (T_w - T(y,t)) e^{-t/t_0} d(t/t_0) \quad (49)$$

After combination of Eqs. 38, 39 and 49, it can be derived that:

$$\frac{T_w - \bar{T}(y)}{T_w - T_b} = 1 - \frac{1}{\Gamma(4/3)} \int_0^{\infty} e^{-(\zeta^3 + \zeta_0^3/\zeta^3)} d\zeta \quad (Pr > 1) \quad (50)$$

where

$$\zeta_0 = \left(\frac{4Pr}{3\sqrt{\pi}}\right)^{1/3} \cdot \left(\frac{y}{2\sqrt{(\nu t_0)}}\right) \quad (51)$$

Time-averaged heat flux through the interface for Pr < 1

The heat flux from the wall into a fluid element encounters approximately a fluid flowing with the bulk velocity if the penetration depth of heat is larger than that of momentum ($Pr < 1$). The heat transfer may then be approximated by an unsteady diffusion of heat into a plug flow. This heat-transfer problem is described by the *classical* differential equation of the surface-renewal theory (Danckwerts, 1951), which also follows from Eq. 33 and $u(y,t)/u_b = 1$:

$$\frac{\partial T(y,t)}{\partial t} = a \frac{\partial^2 T(y,t)}{\partial y^2} \quad (52)$$

The solution to Eq. 52 under the conditions of Eq. 34 is:

$$\frac{T_w - T(y,t)}{T_w - T_b} = \text{erf}\left(\frac{y}{2\sqrt{(at)}}\right) \tag{53}$$

The local instantaneous heat flux from the interface into a single-fluid element is obtained from:

$$q_w(t) = -\lambda\left(\frac{\partial T(y,t)}{\partial y}\right)_{y=0} = \lambda(T_w - T_b)(\pi at)^{-1/2} \tag{54}$$

The local time-averaged heat flux can be obtained using Eqs. 11 and 54:

$$\bar{q}_w = \lambda(T_w - T_b)(at_0)^{-1/2} \tag{55}$$

Combining Eqs. 18 and 55, and $Pr = \nu/a$, it may be stated that:

$$Nu = (f/2)Re\ Pr^{1/2} \quad (Pr < 1) \tag{56}$$

Combining Eqs. 46 and 56 results in:

$$Nu = 0.023\ Re^{0.80}Pr^{1/2} \quad (10^4 \le Re \le 2 \cdot 10^5;\ Pr < 1) \tag{57}$$

This result is in agreement with the fact that, if $Pr < 1$, measured values of the heat-transfer coefficients fit better with an equation, in which the Nusselt number is proportional to $Pr^{1/2}$ (Van der Linden, 1990). Note that Eq. 57 is not valid for heat transfer into a turbulent flow of liquid metals.

Mass Transfer

In the following two sections, equations will be given for the local time-averaged *mass-transfer coefficient* and radial *concentration profile* in the wall region of a turbulent pipe flow. These equations can be derived in a similar way as it has been done for the local time-averaged heat-transfer coefficient and radial temperature profile.

Mass-transfer coefficients

After introducing the dimensionless local time-averaged mass-transfer coefficient or Sherwood number ($Sh = kd/D$), and the Schmidt number ($Sc = \nu/D$), it can be obtained that:

$$Sh = C(f/2)Re\ Sc^{1/3} \quad (Sc > 1) \tag{58}$$

where C is given in Eq. 42, and

$$Sh = (f/2)Re\ Sc^{1/2} \quad (Sc < 1) \tag{59}$$

From Eqs. 42, 46, 58 and 59, it can be obtained that:

$$Sh = 0.021\ Re^{0.80}Sc^{1/3} \quad (10^4 \le Re \le 2 \cdot 10^5;\ Sc > 1) \tag{60}$$

$$Sh = 0.023\ Re^{0.80}Sc^{1/2} \quad (10^4 \le Re \le 2 \cdot 10^5;\ Sc < 1) \tag{61}$$

Time-averaged radial concentration profile in the wall region for $Sc > 1$

In a similar way as the time-averaged radial *temperature* profile of Eq. 50 has been obtained, the following time-averaged radial *concentration* profile in the wall region can be derived:

$$\frac{c_w - \bar{c}(y)}{c_w - c_b} = 1 - \frac{1}{\Gamma(4/3)}\int_0^\infty e^{-(\kappa^3 + \kappa_0^3/\kappa^3)}d\kappa \quad (Sc > 1) \tag{62}$$

where

$$\kappa = \left(\frac{4Sc}{3\sqrt{\pi}}\right)^{1/3} \cdot \left(\frac{y}{2\sqrt{(\nu t)}}\right) \text{ and } \kappa_0 = \left(\frac{4Sc}{3\sqrt{\pi}}\right)^{1/3} \cdot \left(\frac{y}{2\sqrt{(\nu t_0)}}\right) \tag{63}$$

Analogy Between Transfer Processes in Turbulent Pipe Flow

Introduction

The analogies among momentum, heat, and mass transfer have played an important role in the development of heat- and mass-transfer theories for turbulently flowing fluids. Their use has not only been limited to the prediction of heat- and mass-transfer coefficients from the more easier measurable pressure-drop data, but has also been serving as a tool to study the mechanisms of momentum, heat and mass transfer, and of turbulence itself.

In the previous sections, it has been shown that the transfer of momentum, heat and mass in turbulent pipe flow can be described with the ERSR model. It is well known that the momentum flux to the interface, that is, the shear stress exerted on the interface, is described by using the *friction factor*. The heat and mass fluxes to or from the interface, however, are described by using *transfer coefficients*. This difference in approach is traditional in engineering practice, probably due to the fact that originally transport phenomena in turbulent flows were studied by engineers of different disciplines. The early research concerning *momentum* transfer was mainly carried out by civil engineers, who had at that time no professional interest in heat or mass transfer. Investigations on *heat* transfer in turbulent flows were carried out mainly by mechanical engineers, having no professional interest in mass transfer. *Mass* transfer in turbulent flows has been a subject studied by chemical engineers. This diverse background of engineers might have caused the difference in engineering approach of these three transfer processes in turbulent fluid flows.

ERSR analogy among transfer coefficients in turbulent pipe flow

The analogy among momentum, heat, and mass transfer in turbulent pipe flow can be elucidated by introducing a *momentum-transfer coefficient* k_m. This momentum-transfer coefficient for turbulent pipe flow can be defined by:

$$\bar{\tau}_w = k_m(\rho u_b - \rho u_w) \tag{64}$$

where $(\rho u_b - \rho u_w)$ is the axial momentum difference per unit of volume between the bulk of the fluid and the fluid at the pipe wall. As u_w is zero, it may be stated that:

$$\bar{\tau}_w = k_m(\rho u_b) \tag{65}$$

If $u_b \approx \langle u \rangle$ at $Re \geq 10^4$, for example, combination of Eqs. 17 and 65 results in:

$$k_m = (f/2)\langle u \rangle \tag{66}$$

Introducing a dimensionless time-averaged momentum-transfer coefficient, which will be called the Fanning number ($Fa = k_m d/\nu$), Eq. 66 results in:

$$Fa = k_m d/\nu = (f/2)Re \tag{67}$$

The three dimensionless numbers governing the transfer of momentum, heat and mass in turbulent pipe flow can also be defined by:

$$Fa = \frac{k_m \Delta(\rho u)}{\nu \Delta(\rho u)/d} \quad Nu = \frac{\alpha \Delta T}{\lambda \Delta T/d} \text{ and } Sh = \frac{k \Delta c}{D \Delta c/d} \tag{68}$$

Equation 68 shows that each of these dimensionless numbers is equal to the ratio between the total amount of momentum, heat or mass transferred by both *molecular diffusion and forced convection* and the amount of momentum, heat or mass transferred by *molecular diffusion*.

From Eqs. 18, 45, 56, 58, 59 and 67, it is obtained that according to the ERSR model the *transfer equations for turbulent pipe flow* can be written as:

$$Fa = (f/2)Re = Fo^{-1/2} \tag{69}$$

$$Nu = C(f/2)Re\ Pr^{1/3} = CFo^{-1/2}Pr^{1/3} \quad (Pr > 1) \tag{70}$$

$$Nu = (f/2)Re\ Pr^{1/2} = Fo^{-1/2}Pr^{1/2} \quad (Pr < 1) \tag{71}$$

$$Sh = C(f/2)Re\ Sc^{1/3} = CFo^{-1/2}Sc^{1/3} \quad (Sc > 1) \tag{72}$$

$$Sh = (f/2)Re\ Sc^{1/2} = Fo^{-1/2}Sc^{1/2} \quad (Sc < 1) \tag{73}$$

where C follows from Eq. 42.

These equations show that the dimensionless transfer coefficients of momentum (Fa), heat (Nu), and mass (Sh) can be obtained in two independent ways:

- From the friction factor, the Reynolds number, and the transport properties of the fluid.
- From the mean age t_0, the tube diameter, and the transport properties of the fluid.

The *keys* to make Eqs. 69 to 73 operational for the calculation of transfer coefficients are:

- A correlation between the Fanning friction factor f and Re, for example, either Eqs. 25 or 46.
- Values of the mean age t_0 of the fluid elements at the tube wall.

Combination of Eqs. 25 and 69 results in:

$$Fa = Fo^{-1/2} = 0.03683\ Re(\log(Re/7))^{-2} \tag{74}$$

This equation, which holds for fully developed turbulent pipe flow of Newtonian fluids in straight smooth tubes, is shown in Figure 1.

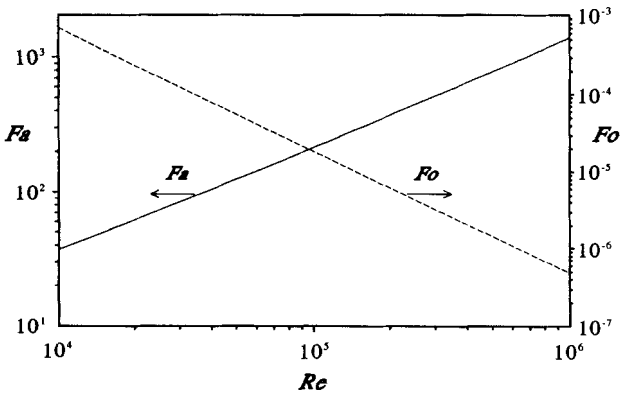

Figure 1. Fanning and Fourier numbers (Eq. 74) vs. Reynolds number for turbulent Newtonian fluid flow through a straight smooth tube.

ERSR analogy among radial profiles of the axial velocity, the temperature and the concentration in the wall region of a turbulent pipe flow

Using Eqs. 24, 45, 50, 51, 58, 62, 63 and 67, and introducing the dimensionless quantities u^0, T^0, and c^0, the ERSR model leads to the *general radial profiles* of the axial velocity, the temperature and the concentration in the wall region of a turbulent pipe flow for $Re \geq 10^4$, $Pr > 1$, and $Sc > 1$ (see also Figure 2):

$$u^0 = 1 - e^{-(y/d)Fa} \text{ and if } C_0 = \frac{\Gamma(4/3)}{\sqrt{\pi}} = 0.5038 \tag{75}$$

$$T^0 = 1 - \frac{1}{\Gamma(4/3)} \int_0^\infty e^{-(\zeta^3 + \zeta_0^3/\zeta^2)} d\zeta \text{ where } \zeta_0 = C_0(y/d)Nu \tag{76}$$

$$c^0 = 1 - \frac{1}{\Gamma(4/3)} \int_0^\infty e^{-(\kappa^3 + \kappa_0^3/\kappa^2)} d\kappa \text{ where } \kappa_0 = C_0(y/d)Sh \tag{77}$$

For values of $Re \geq 10^4$, $Pr < 1$, and $Sc < 1$ the *general radial profiles* of the axial velocity, the temperature and the concentration in the wall region are given by (see Figure 3):

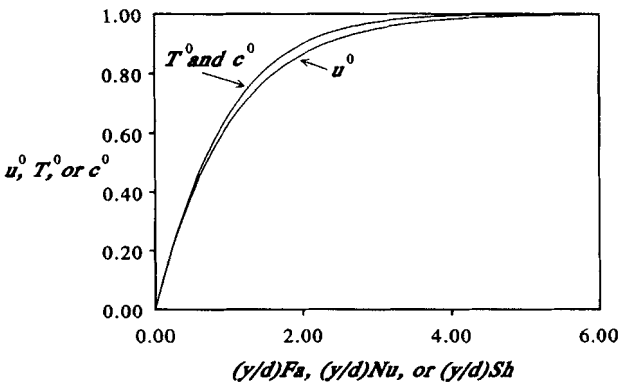

Figure 2. General radial profiles of the axial velocity, temperature and concentration in the wall region of a turbulent pipe flow for values of $Pr > 1$ and $Sc > 1$.

The profiles are calculated with Eqs. 75, 76 and 77, respectively.

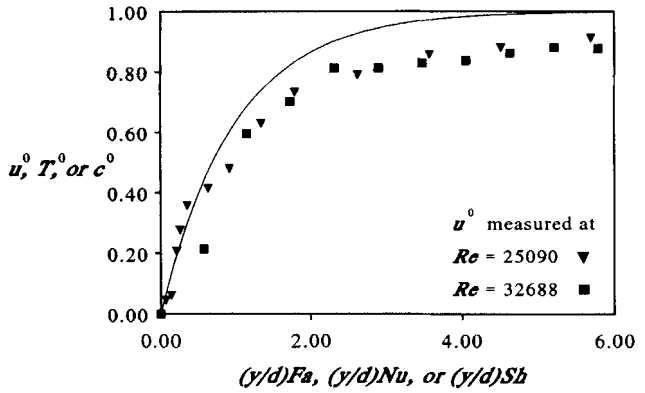

Figure 3. General radial profiles of the axial velocity, temperature and concentration in the wall region of a turbulent pipe flow for values of $Pr<1$ and $Sc<1$.

The profiles are calculated with Eqs. 78, 79 and 80, respectively. The markers refer to local time-averaged axial velocities measured with a laser-Doppler anemometer.

$$u^0 = 1 - e^{-(y/d)Fa} \quad (Re \geq 10^4) \tag{78}$$

$$T^0 = 1 - e^{-(y/d)Nu} \quad (Re \geq 10^4;\ Pr < 1) \tag{79}$$

$$c^0 = 1 - e^{-(y/d)Sh} \quad (Re \geq 10^4;\ Sc < 1) \tag{80}$$

The values of Fa, Nu, and Sh in Eqs. 75 to 80 can be obtained from Eqs. 69 to 73. Further, the definition of the dimensionless distance to the wall $y^0 = (y/d)Fa = (y/d)Re(f/2)$ in the *general velocity profile* is comparable with the definition of the dimensionless distance to the wall $y^+ = (yu^*/\nu) = (y/d)Re\sqrt{(f/2)}$ in the classical universal velocity profile.

Chilton-Colburn analogy

Colburn (1933), and Chilton and Colburn (1934) introduced correlations based on the analogy among momentum, heat, and mass transfer in turbulent pipe flow. They proposed an *empirical* analogy for $Re \geq 10^4$ in long smooth pipes, which can be represented by (Colburn, 1933):

$$j_h = Nu/(Re \cdot Pr^{1/3}) = f/2 \quad (10^4 \leq Re;\ 0.7 \leq Pr \leq 700) \tag{81}$$

where j_h is the *Chilton-Colburn "j factor"* for heat transfer, and by (Chilton and Colburn, 1934):

$$j_d = Sh/(Re \cdot Sc^{1/3}) = f/2 \quad (2 \cdot 10^3 \leq Re \leq 3 \cdot 10^5;\ 0.6 \leq Sc \leq 2{,}500) \tag{82}$$

where j_d is the *Chilton-Colburn "j factor"* for mass transfer. The Colburn (1933) and the Chilton-Colburn analogy (1934) have proved to be very useful since their introduction. Furthermore, the Colburn analogy represents experimental data extremely well over the range in which the empirical correlation is valid (Brodkey and Hershey, 1989).

The ERSR model provides a basis for explaining the Chilton-Colburn analogy for turbulent pipe flow. From Eqs. 70 and 72, it is obtained that for heat and mass transfer in turbulent pipe flow the following equations hold:

$$j_h = C(f/2) \quad (Pr > 1) \tag{83}$$

$$j_d = C(f/2) \quad (Sc > 1) \tag{84}$$

where C is given in Eq. 42.

The Chilton-Colburn j factors for heat and mass transfer derived from the ERSR model differ from those proposed by Chilton and Colburn by less than 10%.

Different types of transfer

The transfer of momentum, heat and mass in turbulent pipe flow can be influenced by additional effects. As a consequence, three different types of transfer rate can be distinguished:

- *Normal* transfer was described in the previous sections by the ERSR model.
- *Enhanced* transfer, due to, for example, chemical reactions in the near-wall fluid or to density gradients and surface-tension gradients, might also be described by Eqs. 69 to 73, provided that an additional *empirical* enhancement factor is introduced. Bakker (1965) and Moens (1972) measured enhancement-factor values of about 2 as a result of surface-tension gradients at an interface. Further, an enlarged roughness of the tube wall may also increase the transfer coefficients (Seidman, 1978).
- *Reduced* transfer, due to, for example, the presence of drag reducers (Duduković, 1988), might also be described by the Eqs. 69 to 73, provided that in these equations f is replaced by the empirical friction factor f_p, where $f_p = f_{dr} \cdot f$, in which f_{dr} is a drag-reduction factor (Fortuin and Klijn, 1982; Musschenga et al., 1991).

Surface-Renewal Measurements Using Laser-Doppler Anemometry

According to the ERSR model, the exchange of momentum, heat and mass between the solid-fluid interface and the core in turbulent pipe flow is governed by the *age distribution* and the *mean age* of the fluid elements at the tube wall. In this section, it will be shown that the distribution and the mean age can be derived from velocity signals measured with a laser-Doppler anemometer (LDA) during turbulent pipe flow, followed by a discrimination procedure to detect the time intervals between two successive surface renewals. These *time intervals* are considered as the *ages* of the fluid elements at the tube wall. The mean value of the *measured* time intervals is indicated as $\bar{\theta}_{exp}$.

It is assumed that the axial velocity signals *measured in time* at a fixed radial position y in the wall region of a turbulent pipe flow are representative of those occurring at all other axial and tangential positions with an equal radial distance y to the wall.

Experimental setup

The setup consists of a 51-mm-ID smooth copper pipe with a total length of 30 m. This pipe has a horizontal, straight section of about 8.5 m, called the *measuring pipe*. There is

sufficient entry and exit length for the turbulent fluid flow to be fully developed in the *test section*. The test section is situated 5.5 m away from the entrance of the measuring pipe. This test section consists of a carefully selected 1.4-m-long glass tube with an inner diameter of 51 mm, in which the velocity of light-scattering particles in the intersection volume of two coherent laser beams of a laser-Doppler anemometer is used to measure the instantaneous local axial fluid velocity. Tap water is used as measuring liquid. The flow rate is controlled by means of valves and rotameters with overlapping ranges for measurements of volume-flow rates ranging from 0.07 to 7 $dm^3 \cdot s^{-1}$ or average fluid velocities ranging from 0.034 to 3.4 $m \cdot s^{-1}$. The actual mass-flow rate is determined by weighing the amount of water leaving the pipe in a measured time interval. The application of this method results in a value of the mass flow rate with an error less than 0.2%. A water manometer is used to measure the pressure drop over a pipe length of 5.89 m. The error in the pressure drop ranges from 0.5 to 5 Pa, depending on the angle of inclination of the manometer.

Light-scattering particles, necessary for measurements with a laser-Doppler anemometer, are supplied from a vessel containing diluted milk using a rotary displacement pump. The diluted milk is injected through an injection port placed 9.75 m upstream of the test section. The concentration of the milk in the turbulent flow is approximately 50 wppm.

Laser-Doppler anemometer

A laser-Doppler anemometer, indicated by LDA and operating in the reference beam mode, was used. This arrangement was chosen for its ease of alignment and the good signal-to-noise ratio in cases where many light-scattering particles are present in the measuring volume. The laser-Doppler anemometer consists of a Spectra Physics 15-mW He-Ne laser ($\lambda = 632.8$ nm) and quality optics, assembled by the Institute of Applied Physics TNO-TU Delft, The Netherlands. In the optical arrangement used, the angle between the two laser beams was 20.96°, which resulted in a measuring volume with a length of 210 μm and a diameter of 39 μm in air. The LDA is mounted on an optical bench, which enables precise movement of the measuring volume in two directions perpendicular to the axis of the tube. Figure 4 shows the test section, the laser-Doppler anemometer and the data-processing equipment. The LDA and the data-processing equipment consist of: a frequency tracker (Type 1077/2/M, made by the Institute of Applied Physics TNO-TU Delft, The Netherlands); an anti-aliasing low-pass filter (type SICOS MF16 dual ETD filter from Difa Measuring Systems, Breda, The Netherlands); an A/D converter (IBM DACA Card); a PC-AT computer; and a tape streamer. All data processing is done by computer, using programs written in FORTRAN and ASSEMBLER. The tape streamer is used to store all the measured velocity signals on tape.

Measurements with the laser-Doppler anemometer

The local instantaneous axial velocity near the tube wall ($y^+ = 36$) in a fully developed turbulent pipe flow was measured using the laser-Doppler anemometer described above. Experimental results obtained at 13 different Reynolds numbers, mentioned in Table 2, refer to temperatures ranging from 280 K to 295 K. During each steady-state measurement, a constant water temperature was maintained. As a consequence, the values of the transport properties, ρ and ν, were constant during such an experiment. The measured results are shown in Table 2.

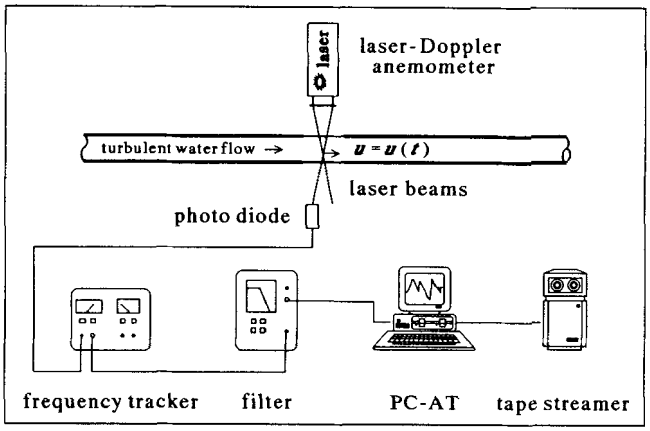

Figure 4. Test section, laser-Doppler anemometer, and data-processing equipment.

It has to be noted that the highest spatial resolution of the laser-Doppler anemometer will be obtained with the shortest dimension of the measuring volume in the radial direction (Van Maanen and Fortuin, 1982, 1983). In this configuration, however, reflection of the laser beams on the tube wall made it impossible to measure axial velocities at a position of $y^+ \leq 36$ at $Re \geq 15 \times 10^3$. Therefore, all the measurements had to be carried out with the longest dimension of the measuring volume in the radial direction.

The proper filter and sample frequency for each Reynolds number were determined from power spectra of velocity data measured at $y^+ = 36$. The low-pass filter frequency was chosen so that most of the laser noise is removed, while the turbulence spectrum remains unchanged. The sample frequency was taken

Table 2. Conditions during Local Instantaneous Axial Velocity Measurements at $y^+ = 36$ in a Turbulent Water Flow through a Horizontal, Straight and Smooth Tube ($d = 51 \cdot 10^{-3}$ m)*

Re 10^3	T K	$10^6\ \nu$ $m^2 \cdot s^{-1}$	t_0 s	$\bar{\theta}_{exp}$ s
12.1	289.3	1.10	1.124	1.163
15.0	281.3	1.38	0.690	0.690
19.5	289.4	1.10	0.562	0.592
24.3	288.8	1.12	0.395	0.412
31.3	291.7	1.04	0.291	0.293
37.2	292.5	1.02	0.228	0.238
40.2	290.3	1.08	0.192	0.190
42.7	292.8	1.01	0.187	0.185
43.4	293.1	1.00	0.184	0.184
49.9	292.8	1.01	0.148	0.198
55.5	288.4	1.13	0.113	0.457
57.3	291.9	1.03	0.118	0.272
59.0	292.8	1.01	0.115	0.280

* The values of t_0 were calculated with Eq. 19. Note that $a = (34.8 \times 10^{-3}) \cdot t_0$, and $k_0 = 1.13$ were chosen in such a way that at $Re = 15 \times 10^3$ $\bar{\theta}_{exp} = t_0$. The same values of $a = (34.8 \times 10^{-3}) \cdot t_0$ and k_0 were used at all other 12 Reynolds numbers. At each Reynolds number, more than 4×10^3 time intervals between successive surface renewals were measured.

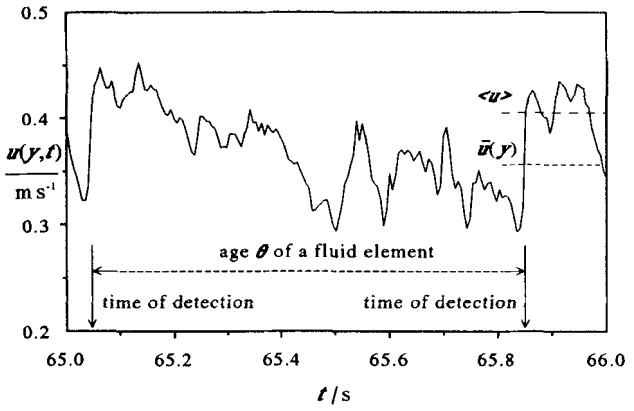

Figure 5. Local instantaneous axial velocities vs. time.

Measured at $Re = 15.0 \times 10^3$, $d = 51 \cdot 10^{-3}$ m, $y^+ = 36$, and $\nu = 1.38 \cdot 10^{-6}$ m^2 s^{-1}, showing two successively detected surface renewals, using $a = (34.8 \times 10^{-3}) \cdot t_0$ and $k_0 = 1.13$. The measured time interval $\theta = 0.80$ s between the two successive renewals is considered as the age of a fluid element at the tube wall.

four times the filter frequency. For each of the Reynolds numbers considered, the total sample time was chosen in such a way that a significant amount of about 4×10^3 surface renewals could be detected in the measured axial velocity signals.

Detection criterion of Blackwelder and Kaplan

In the literature, several criteria for the detection of surface renewals have been formulated (see, for example, Kim et al., 1971; Narahari Rao et al., 1971; Wallace et al., 1972; Strickland and Simpson, 1975; Bogard and Tiederman, 1986; Luchik and Tiederman, 1987; Tiederman, 1988). All these criteria are based on the observation that during the renewal process a sudden increase occurs in the instantaneous local velocity near the wall, such as, the axial velocity, resulting in changes of u', u'^2, and $\partial u'/\partial t$. In applying these criteria to velocity signals measured (see Figure 5), care should be taken to avoid false results caused by the detection criteria itself. A useful way of checking detection criteria is to apply them to synthetic turbulence obtained from a white-noise generator. A conditional average of such a "synthetic velocity signal" vs. the difference $(t - t_d)$ between the time t and the detection times t_d of the surface renewals should be equal to the mean value of the "synthetic velocity signal," because white noise is, of course, not structured. From the velocity signals measured during turbulent pipe flow, a conditionally averaged velocity $\hat{u}$ was calculated and plotted against the difference $(t - t_d)$ between the time t and the detection time t_d of each surface renewal. The *random* velocity fluctuations are averaged out against one another, and the *conditionally averaged* velocity around the detection times remains. The detection procedure described by Blackwelder and Kaplan (1976) fulfills this condition. This detection criterion that is also called the variable interval time averaging (VITA) technique reacts on the fluctuating component of the axial velocity signal crossing the local time-averaged axial velocity $\bar{u}(y)$ in a relatively short time. This corresponds to sharp accelerations or sharp decelerations.

According to the criterion of Blackwelder and Kaplan, a surface renewal occurs if:

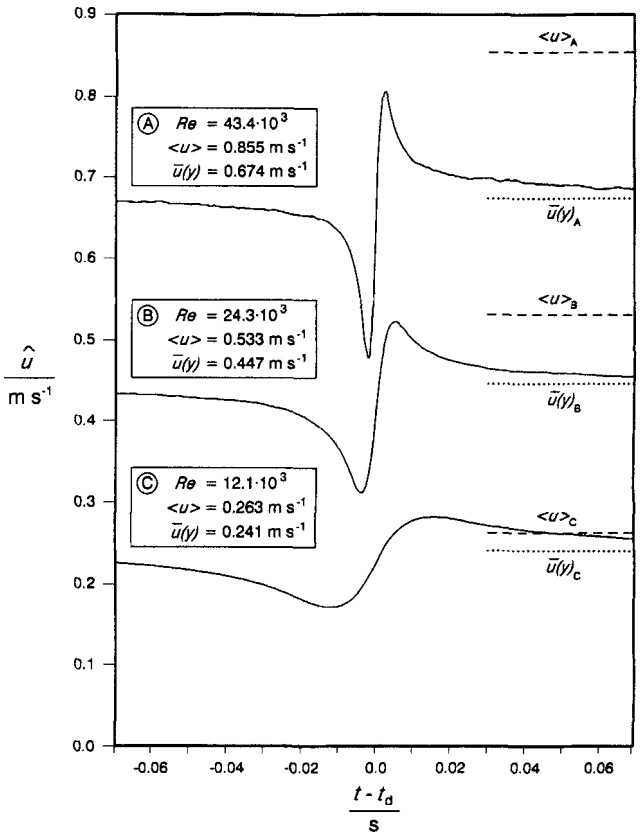

Figure 6. Conditionally averaged axial velocities $\hat{u}$ vs. difference $(t - t_d)$ between time t and detection times t_d of the surface renewals.

The conditionally averaged axial velocities were calculated from local instantaneous axial velocities measured in the wall region of a turbulent pipe flow at $Re = 12.1 \times 10^3$, $Re = 24.5 \times 10^3$, and $Re = 43.4 \times 10^3$, where $d = 51 \times 10^{-3}$ m, $y^+ = 36$, $a = (34.8 \times 10^{-3}) \cdot t_0$, and $k_0 = 1.13$.

$$\frac{\overline{(u')^2}^a - \left[\overline{u'}^a\right]^2}{\overline{(u')^2}^{ent}} \geq k, \quad \text{where } u' = u(y,t) - \bar{u}(y) \tag{85}$$

In Eq. 85 $\overline{\quad}^a$ denotes averaging over a short time of a seconds, and $\overline{\quad}^{ent}$ means averaging over the *entire* signal; k is a dimensionless constant. If this criterion is applied to the local instantaneous axial velocities measured at a fixed position in the wall region, the conditionally averaged axial velocity $\hat{u}$ vs. the difference $(t - t_d)$ between the time t and the detection time t_d of each surface renewal differs significantly from the mean value $\bar{u}$ (Van Maanen and Fortuin, 1982, 1983). The most remarkable aspect of this conditionally averaged axial velocity is the sharp fluid *acceleration* that takes place in the wall region at the time of the renewal process (see Figure 6). Further, *decelerations* will not be counted as a renewal process.

Specification of the averaging time a and the threshold level k

Application of the detection criterion requires the specification of two parameters: the *averaging time a* and the di-

mensionless *threshold level k*. The number of detected events is affected by the values of the averaging time and the threshold level. Fully objective values of the averaging time a and threshold level k cannot be found, because no calibration data are available: the number of surface renewals we *should* have to find under any given set of experimental conditions is unknown. The detection criterion can only give well-defined, objective values of the time intervals, if a and k have objective values. Values of k frequently used in the literature range from 0.2 to 1.6 (see, for example, Johansson and Alfredsson, 1982).

The *averaging time a* must be of the same order as the short time interval, in which the sudden velocity increase during the surface renewal occurs. If the averaging time is too short, more than one event may be detected on one slope. On the other hand, if the averaging time a is too large, the sharp acceleration during the surface renewal may disappear in random velocity fluctuations. The value of the short time interval, in which the axial velocity increase occurs during a surface renewal, is influenced by the frequencies of the fluctuating velocity signal, which depend on the Reynolds number (Figure 6). Therefore, if the Reynolds number is changed, the averaging time a has to be changed too. It is common in the literature (for example, Blackwelder and Kaplan, 1976) to scale the averaging time with so-called *inner* variables, resulting in a *dimensionless averaging time* $t^+ = a/(\nu/u^{*2})$. Values of t^+ used in the literature vary from 4 to 32 (see Johansson and Alfredsson, 1982). Musschenga et al. (1990) have recently shown that scaling of the averaging time a with the mean age $t_0 = (\nu/u^{*2}) \cdot 2/f$, instead of with inner variables (ν/u^{*2}), results in a value of a/t_0, which appears to be independent of the Reynolds number.

In the present study, the averaging time a is scaled with the mean age t_0. A value of the dimensionless averaging time t^+, used by several authors including Blackwelder and Kaplan (1976) is $t^+ = a/(\nu/u^{*2}) = 10$, which results in $a = 24$ ms at $Re = 15.0 \times 10^3$. According to Eq. 19, $t_0 = 0.69$ s at $Re = 15.0 \times 10^3$ (see Table 2); as a consequence, the dimensionless averaging time can be ascribed a value $a = (34.8 \times 10^{-3}) \cdot t_0$.

The *threshold level k* is given by such a value $k = k_0$ that for an arbitrary reference Reynolds number ($Re = 15.0 \times 10^3$) the measured mean age of the fluid elements at the tube wall $\bar{\theta}_{exp}$ equals the theoretical value t_0. If a/t_0 and k_0 are independent of the Reynolds number, the mean ages $\bar{\theta}_{exp}$ at the other Reynolds numbers can be obtained from the measured velocity signals using the same values of a/t_0 and k_0 as has been applied at $Re = 15.0 \times 10^3$. The experimental results obtained according to this procedure will be compared with those calculated with the ERSR model.

Results and Discussion

The mean ages presented in Table 2 were obtained in two different ways. According to the first method, $\bar{\theta} = t_0$ was calculated from values of f and Re using Eq. 19. According to the second method, $\bar{\theta}_{exp}$ was obtained from velocity signals measured with a laser-Doppler anemometer. For each of the Reynolds numbers, the distribution and the mean age $\bar{\theta}_{exp}$ of the fluid elements at the tube wall were determined from the measured velocity signals after applying the detection criterion represented as Eq. 85 and an additional condition of positive slope, using the averaging time $a = (34.8 \times 10^{-3}) \cdot t_0$ and the threshold level $k = k_0 = 1.13$ (Musschenga et al., 1990).

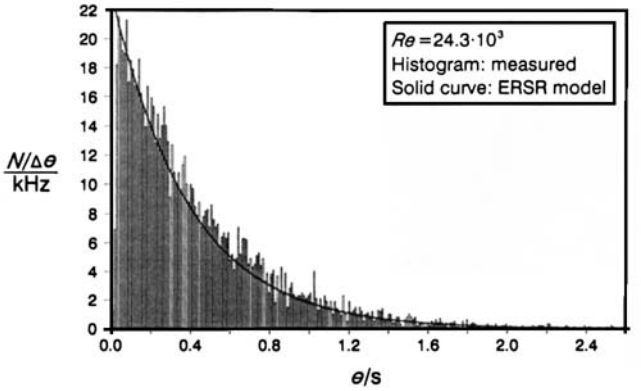

Figure 7. Age distribution determined in a turbulent pipe flow at $Re = 24.3 \times 10^3$, $d = 51 \times 10^{-3}$ m, $y^+ = 36$, and $\nu = 1.12 \times 10^{-6}$ m$^2 \cdot$s^{-1}.

The histogram represents the age distribution obtained from velocity signals measured with a laser-Doppler anemometer, using $a = (34.8 \times 10^{-3}) \cdot t_0$, $k_0 = 1.13$, $\Delta\theta = 0.01$ s, $N_0 = 9{,}182$, and $t_0 = 0.395$ s. The solid curve represents the age distribution calculated from f and Re with Eqs. 19, 25 and 87 of the ERSR model.

Measured vs. calculated age distributions of fluid elements at the tube wall

In Figure 5, a typical example is given of the signals representing the local instantaneous axial velocities measured at $Re = 15.0 \times 10^3$ and $T = 15$°C. The time interval between the two successively detected surface renewals in this figure may be considered as the age θ of a fluid element at the tube wall. For the production of the results presented in Table 2, more than 50,000 time intervals were measured.

In Figures 7–9, the age distributions obtained from measurements at three different Reynolds numbers are represented as *histograms*. In these figures, the values of $N/\Delta\theta$ have been plotted against the age θ. The *solid curves* in Figures 7–9 represent the age distributions calculated from the friction factor and the Reynolds number with the ERSR model. The distri-

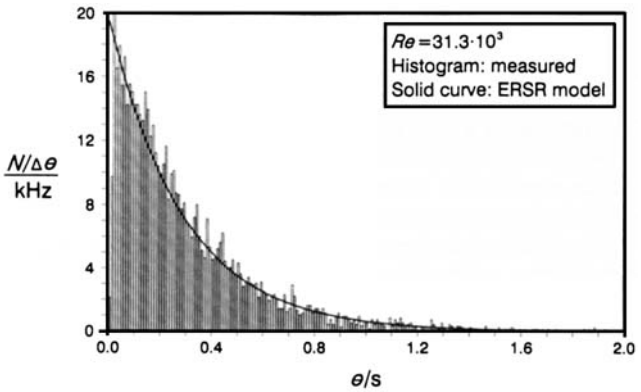

Figure 8. Age distribution determined in a turbulent pipe flow at $Re = 31.3 \times 10^3$, $d = 51 \times 10^{-3}$ m, $y^+ = 36$, and $\nu = 1.04 \times 10^{-6}$ m$^2 \cdot$s^{-1}.

The histogram represents the age distribution obtained from velocity signals measured with a laser-Doppler anemometer, using $a = (34.8 \times 10^{-3}) \cdot t_0$, $k_0 = 1.13$, $\Delta\theta = 0.01$ s, $N_0 = 5{,}759$, and $t_0 = 0.291$ s. The solid curve represents the age distribution calculated from f and Re with Eqs. 19, 25 and 87 of the ERSR model.

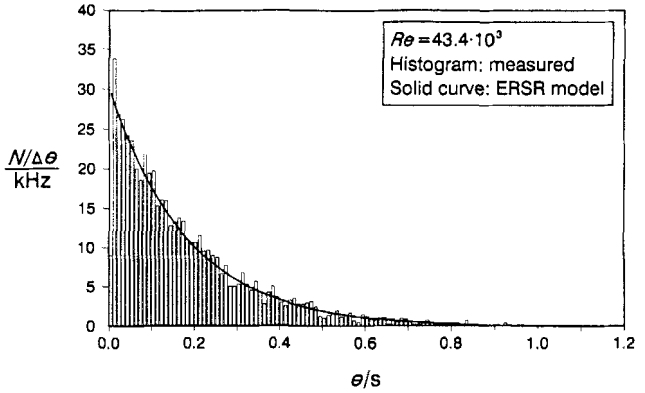

Figure 9. Age distribution determined in a turbulent pipe flow at $Re = 43.4 \times 10^3$, $d = 51 \times 10^{-3}$ m, $y^+ = 36$, and $\nu = 1.00 \times 10^{-6}$ m$^2 \cdot$s^{-1}.

The histogram represents the age distribution obtained from velocity signals measured with a laser-Doppler anemometer, using $a = (34.8 \times 10^{-3}) \cdot t_0$, $k_0 = 1.13$, $\Delta\theta = 0.01$ s, $N_0 = 5{,}595$, and $t_0 = 0.184$ s. The solid curve represents the age distribution calculated from f and Re with Eqs. 19, 25 and 87 of the ERSR model.

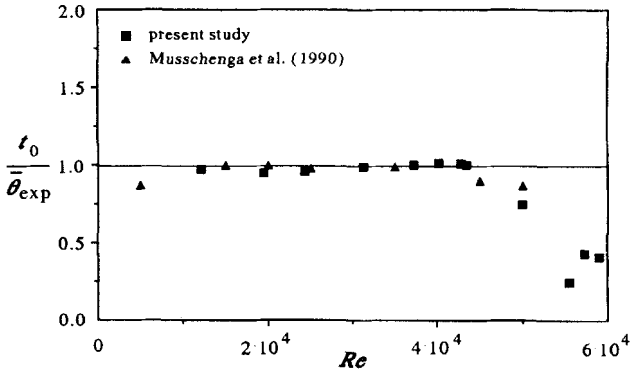

Figure 10. The ratio $t_0 / \bar{\theta}_{exp}$ in turbulent pipe flow vs. Reynolds number where $d = 51 \times 10^{-3}$ m, $y^+ = 36$, $a = (34.8 \times 10^{-3}) \cdot t_0$, and $k_0 = 1.13$.

butions according to the ERSR model were obtained as follows. Denoting the abscissa of the middle point of the horizontal line at the top of each bar in the histogram by θ and the total number of the detected time intervals by N_0, the number N of the detected time intervals ranging from $(\theta - \Delta\theta/2)$ to $(\theta + \Delta\theta/2)$ can be obtained by integration of Eq. 3 between the boundaries mentioned. This results in:

$$N = N_0 e^{-\theta/t_0} 2\sinh\left(\frac{1}{2}\Delta\theta/t_0\right) \tag{86}$$

If $\Delta\theta/t_0 \leq 0.25$, Eq. 86 may be approximated by:

$$N/\Delta\theta = (N_0/t_0) e^{-\theta/t_0} \tag{87}$$

Figures 7-9 show a good agreement between the histograms representing age distributions measured with a laser-Doppler anemometer and the solid curves representing distributions calculated from f and Re with the ERSR model. It has to be noted that in the derivation of Eq. 3, the time interval needed for the renewal of a fluid element at the tube wall is neglected. The renewal of a fluid element, however, requires a *short time interval*, the value of which depends on the Reynolds number. At the experiments presented in Table 2, values between 0.02 s and 0.05 s were approximately obtained. As a consequence, the small difference between the measured and calculated age distributions during the time interval between 0 and 0.02 s to 0.05 s, in Figures 7-9, can be expected.

Comparison between the values of $\bar{\theta}_{exp}$ and t_0

In Figure 10, the ratio $t_0/\bar{\theta}_{exp}$ determined at the conditions mentioned in Table 2 is plotted against the Reynolds number. This figure shows that at Reynolds numbers ranging from 5.0×10^3 to 43.4×10^3, the mean ages of the fluid elements at the tube wall *calculated* from f and Re with the ERSR model (Eq. 19) agree quantitatively with those *measured* with a laser-Doppler anemometer in turbulent pipe flow. Further, it has appeared that the measured values of the mean time intervals $\bar{\theta}_{exp}$ at $Re > 43.4 \times 10^3$ are larger than the values of t_0 calculated from f and Re with the ERSR model. This is probably due to the *measured* values, because at increasing Reynolds numbers the ratio between the length of the LDA measuring volume and the boundary-layer thickness increases. As a consequence, the velocity signals obtained at these larger Reynolds numbers refer to instantaneous velocities averaged over a considerable part of the boundary layer. It can be expected that at these larger Reynolds numbers ($Re > 43.4 \times 10^3$), time intervals between two successive surface renewals which occur immediately after each other cannot be distinguished from the "background turbulence," so that the measured mean ages $\bar{\theta}_{exp}$ will be larger than the calculated values t_0. The results concerning $t_0/\bar{\theta}_{exp}$ vs. Re presented in Figure 10 show this deviation between t_0 and $\bar{\theta}_{exp}$ at $Re > 43.4 \times 10^3$.

From the results obtained from laser-Doppler anemometer measurements, it may be concluded that at $5.0 \times 10^3 \leq Re \leq 43.4 \times 10^3$, both the *distribution* and the *mean value* of the ages of the fluid elements at the tube wall closely agree with those calculated with Eqs. 19 and 87 of the ERSR model.

The agreement between the values of the *heat-transfer coefficients*, obtained with the ERSR model and those calculated with the Colburn correlation, discussed earlier, shows that Eqs. 19 and 87 probably also hold for $Re > 43 \times 10^3$.

The measured *random* age distributions confirm the investigations of Van Maanen and Fortuin (1982, 1983) and verify Danckwerts' (1951) assumptions concerning the random-age distribution of fluid elements at the interface in a turbulent fluid flow. Further, it was found that experiments with drag reducers carried out with diluted aqueous polymer solutions (20 wppm Separan AP-30) showed that the age distribution of the fluid elements at the tube wall is still random and that the mean age is *increased* by the addition of a drag reducer. This increased mean age agrees quantitatively with the mean age calculated with Eq. 19 of the ERSR model, provided that the friction factor f for Newtonian fluids is replaced by the measured value f_p for the polymer solution. Then, the mean age $\bar{\theta}_{exp}$ is obtained from velocity signals using the same values of $a = (34.8 \times 10^{-3}) \cdot t_0$ and $k_0 = 1.13$ as for the above-mentioned Newtonian fluids are applied (Musschenga et al., 1991).

Conditionally averaged axial velocities

In Figure 6, the conditionally averaged axial velocities $\hat{u}$ measured around the detection times of the surface renewals are plotted against the difference $(t-t_d)$ between the time t and the detection time t_d. At three different Reynolds numbers and at $y^+=36$, the curves A, B, and C were obtained. The measured local time-averaged velocities are indicated by $\bar{u}(y)$. The three curves show that during a *surface renewal*, the conditionally averaged axial velocity $\hat{u}$ in the wall region suddenly increases from $\hat{u}<\bar{u}(y)$ via $\hat{u}=\bar{u}(y)$ to a value close to the average velocity $<u>$ of the fluid in the tube. These experimental results support the assumption made earlier that at a fixed position at the tube wall the near-wall fluid can suddenly be renewed by an inrushing fluid element with a velocity that is approximately equal to that of the fluid in the turbulent core.

Comparison with Literature Data

In this section, some of the results obtained with the ERSR model will be compared with experimental data and correlations in the literature.

Mean age of the fluid elements at the tube wall

Transfer rates can be predicted using a surface-renewal model, if the characteristic renewal frequency n_0 of the fluid elements at the wall is known as a function of the Reynolds number. Generally, the renewal frequency n_0, that is, the reciprocal value of the mean age t_0 of the fluid elements at the tube wall in turbulent pipe flow, is obtained from experimental data of Meek (1972), for example. However, there is confusion about the relationship between the values of the mean age and the Reynolds number. The possible relationship between the surface renewal and sublayer structures inspired a number of investigators including Kline et al. (1967), Meek (1972), Pinczewski and Sideman (1974), and Luchick and Tiederman (1987), to scale the measured mean ages $\bar{\theta}_{exp}$ with ν/u^{*2}, consisting of so-called *inner* variables. They state that $\bar{\theta}_{exp}$ becomes independent of the Reynolds number after division by ν/u^{*2}. Other investigators, such as Rao et al. (1971), Blackwelder and Kaplan (1976), Lu and Willmarth (1973), and Cantwell (1981), have the opinion that $\bar{\theta}_{exp}$ can be scaled with δ/U_∞, consisting of so-called *outer* variables. In addition, Alfredsson and Johansson (1984) suggest that $\bar{\theta}_{exp}$ can be scaled with $[(\nu/u^{*2})(\delta/U_\infty)]^{1/2}$, called *mixed* variables.

Despite the numerous studies of the surface-renewal events, no answer is found in the literature concerning the proper scaling of $\bar{\theta}_{exp}$. However, Musschenga et al. (1990) have shown that the scaling of $\bar{\theta}_{exp}$ with t_0, where

$$t_0=\left(\frac{1}{2}f\cdot Re\right)^{-2} d^2/\nu=(\nu/u^{*2})\cdot 2/f \tag{88}$$

instead of with inner variables or outer variables results in a value of $\bar{\theta}_{exp}/t_0$, which appears to be independent of the Reynolds number in the range $5.0\times10^3\le Re\le43.4\times10^3$. The different scaling procedures are summarized in Table 3.

In Figure 11, the experimental data of Meek (1972) concerning the mean ages in turbulent pipe flow have been plotted against the Reynolds number. These mean ages are also called

Table 3. Scaling Procedures for Values of the Mean Age $\bar{\theta}_{exp}$ Measured in Turbulent Pipe Flow

Scaling Procedure	Scaling with	Calculated with
Inner Variables	ν/u^{*2}	$\dfrac{d^2/\nu}{(f/2)Re^2}$
Outer Variables	$d/<u>$	$\dfrac{d^2/\nu}{Re}$
Mixed Variables	$[(\nu/u^{*2})(d/<u>)]^{1/2}$	$\dfrac{d^2/\nu}{\sqrt{(f/2)}Re^{3/2}}$
ERSR model	t_0	$\dfrac{d^2/\nu}{(f/2)^2Re^2}$

mean sublayer periods or reciprocal values of burst frequencies. Because the time intervals given by Meek are made dimensionless with u^* and ν, and the conditions under which these mean ages were measured are not fully specified in his article, these data can only be compared with our results if our measured mean ages $\bar{\theta}_{exp}$ are represented in a similar way. Therefore, the dimensionless parameter $\theta^+=u^*\sqrt{(\bar{\theta}_{exp}/\nu)}$ is plotted against Re in Figure 11. According to the ERSR model, the dimensionless parameter $u^*\sqrt{(\bar{\theta}_{exp}/\nu)}$ can be represented by $u^*\sqrt{(t_0/\nu)}$. Combining Eqs. 17 and 19 results in:

$$\theta^+=u^*\sqrt{(t_0/\nu)}=\sqrt{(2/f)} \tag{89}$$

Combination of Eqs. 25 and 89 leads to:

$$\theta^+=u^*\sqrt{(t_0/\nu)}=5.0882\log(Re)-4.300 \tag{90}$$

From Eq. 90 it is obtained that according to the ERSR model, a linear relationship is expected between the variables plotted in Figure 11. This linear relationship closely agrees with our experimental results in the range $5.0\times10^3\le Re\le43.4\times10^3$. Further, it is found from this figure that the theoretical solid line "agrees" with the "cloud" of experimental data presented

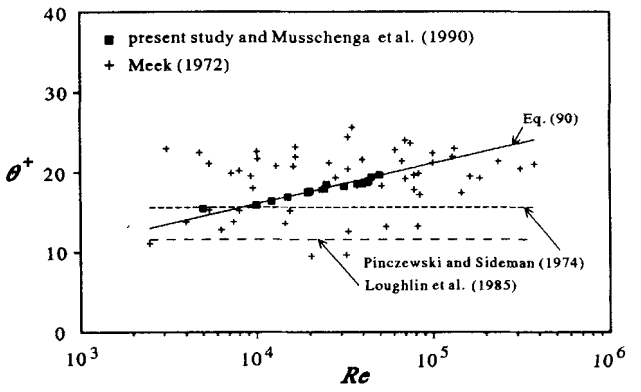

Figure 11. Measured values of the dimensionless parameter $\theta^+ = u^*\sqrt{(\bar{\theta}_{exp}/\nu)}$ vs. Reynolds number.

The solid line represents Eq. 90 calculated with the ERSR model. The horizontal dashed lines represent the dimensionless parameter values proposed by Pinczewski and Sideman (1974), $\theta^+=u^*\sqrt{(\bar{\theta}_{exp}/\nu)}=15.6$, and Loughlin et al. (1985), $\theta^+=u^*\sqrt{(\bar{\theta}_{exp}/\nu)}=11.6$

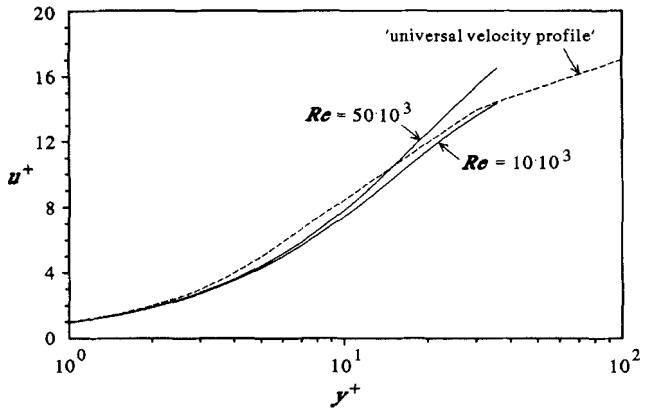

Figure 12. Universal velocity profile in the wall region of a turbulent Newtonian pipe flow.

The values of u^+ against y^+ denoted by the dashed curve are plotted according to Eqs. 91, 92 and 93. The solid curves were calculated with Eq. 28 of the ERSR model using Eq. 25.

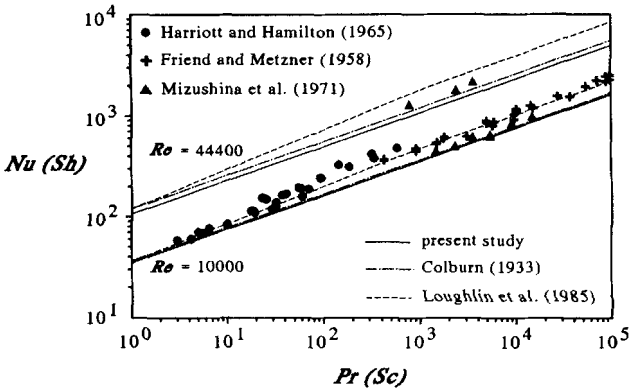

Figure 13. Experimental and calculated values of Nusselt and Sherwood number as a function of Prandtl or Schmidt number at $Re = 10.0 \times 10^3$ and 44.4×10^3.

The solid lines represent values of *Nu* or *Sh* calculated with Eq. 45 or 58 of the ERSR model for values of $Pr > 1$ or $Sc > 1$. In the two cases, Eqs. 25 and 42 were applied. The dashed-dotted lines represent values of *Nu* calculated with Eq. 48 of Colburn (1933). The dashed lines represent Eq. 94 of Loughlin et al. (1985). Experimental data used are by Friend and Metzner (1958), Harriott and Hamilton (1965), and Mizushina et al. (1971).

in the literature. The upper horizontal dashed line in Figure 11 refers to the dimensionless mean ages proposed by Pinczewski and Sideman (1974), and the lower one was calculated by Loughlin et al. (1985). These authors assumed that the value of $u^*\sqrt{(\bar{\theta}_{exp}/\nu)}$ is independent of the Reynolds number. It can be seen that the dimensionless parameter proposed by Pinczewski and Sideman (1974) and that of Loughlin et al. (1985) do not agree with the experimental values of this parameter.

Axial velocity profile in the wall region

In Figure 12, the velocity profiles in the wall region of a turbulent pipe flow calculated with Eqs. 25 and 28 are plotted as solid curves. The dashed curve in this figure represents the "universal velocity profile" for turbulent flow of Newtonian fluids in smooth tubes. This semi-empirical velocity profile is calculated with the following correlations of Perry and Green (1984):

$$u^+ = y^+ \quad \text{for} \quad 0 < y^+ \leq 5 \tag{91}$$

$$u^+ = -3.05 + 5.00 \ln(y^+) \quad \text{for} \quad 5 < y^+ \leq 30 \tag{92}$$

$$u^+ = 5.5 + 2.5 \ln(y^+) \quad \text{for} \quad y^+ > 30 \tag{93}$$

From Eqs. 25 and 28, and Figure 12, it can be obtained that according to the ERSR model a plot of u^+ against y^+ results in a velocity profile that is slightly dependent on the Reynolds number. Close to the wall, however, the calculated profiles quantitatively agree with the semi-empirical "universal velocity profile." Further, it has to be noted that according to the ERSR model, the *general velocity profile* (u^0 against y^0) is independent of the Reynolds number.

Heat- and mass-transfer coefficients

In Figure 13, transfer coefficients calculated with the ERSR model are compared with the experimental data of Friend and Metzner (1958), Harriott and Hamilton (1965), and Mizushina et al. (1971). In this figure, values of the Nusselt or Sherwood number are plotted against the Prandtl or Schmidt number for two different values of the Reynolds number. The solid lines represent values of the Nusselt or Sherwood number calculated with the ERSR model using Eq. 45 or 58 for values of $Pr > 1$ or $Sc > 1$. In both cases, Eqs. 25 and 42 were applied. The dashed-dotted lines represent values of the Nusselt number calculated with the well-known correlation (Eq. 48) of Colburn (1933). The dashed lines represent the Sherwood numbers calculated with the correlation presented by Loughlin et al. (1985):

$$St = \frac{Sh}{Re\,Sc} = \frac{0.023\ Re^{-0.2}}{1 + 1.93\ Re^{-0.1}(Sc^{2/3} - 1)}$$

$$(10^4 \leq Re \leq 2 \times 10^5;\ 0.5 < Sc < 10^4) \tag{94}$$

From Figure 13, it can be seen that the values of the Nusselt and Sherwood number calculated from f and Re with the ERSR model agree with both the correlation of Colburn (1933) and the experimental data of Mizushina et al. (1971). The experimental results of Mizushina et al. (1971) were obtained from mass-transfer measurements at a smooth wall applying an electrochemical method without gradients of density and surface tension in the fluid at the tube wall. Harriott and Hamilton (1965), however, measured larger values of the mass-transfer coefficients at a tube wall. This is probably due to the fact that their measurements refer to a tube wall covered with benzoic acid dissolving in water. Such a transfer process might increase the roughness of the wall and might also cause density gradients and surface-tension gradients in the near-wall fluid. These phenomena can lead to an enhanced mass-transfer rate, as described earlier, and will result in larger measured values of the mass-transfer coefficients. A similar phenomenon might occur, if heat-transfer coefficients are measured with large temperature gradients at the tube wall.

The semitheoretical equation of Loughlin et al. (1985), Eq. 94, which can also be derived from a correlation by Friend and Metzner (1958) or from a correlation by Reichardt (1951),

was obtained with a *surface-rejuvenation model.* The mean ages by Loughlin et al. (1985), however, are much smaller than both the mean ages in the θ^+ values of Meek (1972) and the mean ages in the θ^+ values measured by us (see Figure 11). The smaller mean-age values of Loughlin et al. will lead to higher values of the heat- and mass-transfer coefficients, which Loughlin et al. compensate by *assuming* an unreplenished layer of fluid at the tube wall with an average "thickness" of $y^+ = 5$. Loughlin et al. stated that the thickness of the unreplenished layer of fluid is based on the work of Popovich and Hummel (1967).

Time-averaged radial profiles of temperature and concentration in the wall region (Pr > 1, Sc > 1)

In this section, the time-averaged radial profiles of the temperature and the concentration in the wall region (Eqs. 50 and 62, respectively) are compared with the experimental data and the profiles obtained by Loughlin et al. (1985).

From Eqs. 19, 43, and 50, the following dimensionless quantity is calculated:

$$T^+ = \frac{T_w - \bar{T}(y)}{\bar{q}_w} \rho c_p u^* = \frac{Pr^{2/3}}{C\sqrt{(f/2)}} \times \left[1 - \frac{1}{\Gamma(4/3)} \int_0^\infty e^{-(\zeta^3 + \zeta_0^3/\zeta^2)} d\zeta \right] \quad (95)$$

The value of ζ_0 can be obtained from Eqs. 19 and 51:

$$\zeta_0 = \left[\frac{Pr}{6\sqrt{\pi}} \right]^{1/3} \cdot \left[\frac{f}{2} \right]^{1/2} \cdot y^+ \quad (96)$$

The integral in Eq. 95 can be solved numerically as function of ζ_0.

From the time-averaged concentration profile (Eq. 62), a similar dimensionless quantity c^+ can be calculated:

$$c^+ = \frac{c_w - \bar{c}(y)}{\bar{N}_{Aw}} u^*$$

where

$$\bar{N}_{Aw} = CD(c_w - c_b)(\nu t_0)^{-1/2} Sc^{1/3} \quad (97)$$

Combination of Eqs. 18, 62, and 97, and the definitions of Sc, u^*, and C result in:

$$c^+ = \frac{Sc^{2/3}}{C\sqrt{(f/2)}} \left[1 - \frac{1}{\Gamma(4/3)} \int_0^\infty e^{-(\kappa^3 + \kappa_0^3/\kappa^2)} d\kappa \right] \quad (98)$$

where

$$\kappa_0 = \left[\frac{Sc}{6\sqrt{\pi}} \right]^{1/3} \cdot \left[\frac{f}{2} \right]^{1/2} \cdot y^+ \quad (99)$$

In Figure 14, values of T^+ and c^+ are plotted against y^+ for several Prandtl or Schmidt numbers. The solid curves in this figure are obtained from Eqs. 95 and 98, derived from the ERSR model. The friction factor is calculated from Eq. 25 and $Re = 10^4$. In the *wall region*, these solid dimensionless

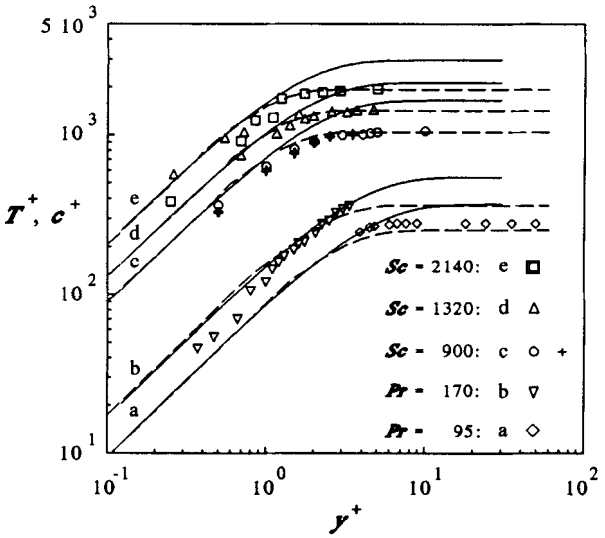

Figure 14. Experimental and calculated T^+ and c^+ profiles in a turbulent pipe flow.

The solid curves refer to Eqs. 95 and 98 from the ERSR model for $Re = 10^4$. The experimental data and the dashed curves refer to Figure 2 of the article by Loughlin et al. (1985). In the wall region, the profiles calculated with the ERSR model agree with those of Loughlin et al. (1985).

temperature and concentration profiles agree with the dashed curves obtained by Loughlin et al. (1985). This result is interesting, because Loughlin et al. (1985) stated that the unreplenished layer of fluid at the tube wall with an average thickness $y^+ = 5$ plays a significant role in describing the mechanisms of heat and mass transfer for values of $Sc > 5$. In the ERSR model, however, it is assumed that the fluid elements at the tube wall are renewed completely. Furthermore, the time-averaged heat- and mass-transfer coefficients calculated with the ERSR model, which are related to the time-averaged radial profiles of the temperature and the concentration in the near-wall fluid, agree within 10% with the well-known empirical correlation of Chilton and Colburn (1933, 1934), and the experimental results of Mizushina et al. (1971) where no density gradients and surface-tension gradients occur.

Another factor to be taken into account is that the T^+ and c^+ profiles of Loughlin et al. (1985) were obtained by coupling their model for the wall region with a eddy-diffusivity model for the turbulent core. The T^+ and c^+ profiles calculated with the ERSR model, however, are derived using a model for the wall region only.

The experimental data in Figure 14 were obtained from Figure 2 of the work of Loughlin et al. (1985).

Conclusions

Investigations in the wall region of a turbulent pipe flow with a laser-Doppler anemometer have shown that the time intervals between successive *surface renewals* are distributed *randomly*. The *mean age* of the fluid elements at the tube wall calculated from the friction factor and the Reynolds number with the ERSR model is equal to the *mean time interval* between successive renewals measured with a laser-Doppler anemometer at $5.0 \times 10^3 \leq Re \leq 43.4 \times 10^3$, using the detection criterion of Blackwelder and Kaplan with an additional condition of

positive slope and suitable values of the averaging time $a=(34.8\times10^{-3})\cdot t_0$, and the threshold level $k_0=1.13$.

The agreement between the values of the heat-transfer coefficients obtained with the ERSR model and those calculated with the Colburn correlation shows that the ERSR model probably also holds for $Re>43\times10^3$.

According to the ERSR model, the *general radial profiles* of the axial velocity, the temperature and the concentration in the wall region are independent of the Reynolds number (see Figures 2 and 3), and the *universal velocity profile* is affected by the Reynolds number (see Figure 12).

The time-averaged radial profile of the *axial velocity* in the *wall region* calculated with the ERSR model and represented in the u^+ against y^+ notation agrees with the correlations for the semi-empirical universal velocity profile presented in the literature.

Heat- and mass-transfer coefficients derived from the ERSR model for turbulent pipe flow agree with both the experimental data of Mizushina et al. (1971) and with results calculated from the correlations of Colburn (1933) and Chilton and Colburn (1934). For shear-bounded turbulent flows, the Nusselt (or Sherwood) number is proportional to the Prandtl (or Schmidt) number raised to a power 1/3 for $Pr>1$ ($Sc>1$) or 1/2 for $Pr<1$ ($Sc<1$).

The dimensionless T^+ and c^+ profiles in the wall region calculated from the ERSR model agree with the results obtained by Loughlin et al. (1985), despite the fact that no unreplenished layer of near-wall fluid is assumed in the ERSR model.

The introduction of a Fanning number for momentum transfer ($Fa=k_m d/\nu$) elucidates the analogy among momentum, heat, and mass transfer in turbulent pipe flow. The Fanning number for *momentum* transfer is comparable with the Nusselt number for *heat* transfer and the Sherwood number for *mass* transfer.

The ERSR model provides a basis for explaining the Chilton-Colburn analogy. The factors j_h for heat transfer and j_d for mass transfer also follow from the ERSR model.

The relationship between the friction factor and the Reynolds number is the one and only correlation needed for a quantitative prediction of the momentum, heat- and mass-transfer coefficients in turbulent pipe flow.

Acknowledgment

The authors wish to thank The Netherlands Foundation for Chemical Research (SON) for the financial aid from The Netherlands Organisation for Scientific Research (NWO). We also would like to thank Messrs. J. Ellenberger, J. Zoutberg, Th. J. A. M. Nass, D. P. de Zwarte, and W. H. Buster of the University of Amsterdam for their technical assistance; Mr. E. Grolman for programming the system for the digital signal analysis; and Messrs. E. P. S. Schouten and W. Visser for their contribution to the experimental part of this study.

Notation

a = thermal diffusivity ($a=\lambda/\rho c_p$), $m^2\cdot s^{-1}$
a = averaging time in Eq. 85, s
c_b = bulk concentration, $mol\cdot m^{-3}$
c_p = heat capacity at constant pressure, $J\cdot kg^{-1}\cdot K^{-1}$
c_w = concentration in the fluid at the interface, $mol\cdot m^{-3}$
$\bar{c}(y)$ = local time-averaged concentration, $mol\cdot m^{-3}$
c^0 = dimensionless concentration in the wall region [$c^0=(c_w-\bar{c}(y))/(c_w-c_b)$], 1
c^+ = dimensionless concentration {$c^+=[c_w-\bar{c}(y)]u^*/\bar{N}_{Aw}$}, 1
C = constant defined in Eq. 42, 1
C_0 = constant defined in Eq. 75
d = tube diameter, m
D = diffusivity, $m^2\cdot s^{-1}$
f = Fanning friction factor for Newtonian fluids [$f=\bar{\tau}_w/(\rho<u>^2/2)$], 1
f_{dr} = drag-reduction factor ($f_{dr}=f_p/f$), 1
f_p = friction factor for aqueous solutions of drag-reducing polymers, 1
$F(y,t)$ = local instantaneous physical quantity in a fluid element at a distance y to the tube wall
$\bar{F}(y)$ = local time-averaged physical quantity
$\bar{F}(y,\theta)$ = local age-averaged physical quantity
j_d = Chilton and Colburn j factor for mass transfer in Eq. 82, 1
j_h = Chilton and Colburn j factor for heat transfer in Eq. 81, 1
$J_w(t)$ = local instantaneous flux at the tube wall
$\bar{J}_w$ = local time-averaged flux at the tube wall
k = mass-transfer coefficient, $m\cdot s^{-1}$
k_m = momentum-transfer coefficient defined in Eq. 64, $m\cdot s^{-1}$
k = threshold level in Eq. 85, 1
k_0 = fixed value of the threshold level k, 1
$L\{F(y,t)\}$ = Laplace transform of $F(y,t)$
n_0 = characteristic surface-renewal frequency calculated with the ERSR model ($n_0=1/t_0$), Hz
N = number of time intervals measured between $(\theta-\Delta\theta/2)$ and $(\theta+\Delta\theta/2)$, 1
$\bar{N}_{Aw}$ = local time-averaged mass flux at the interface, $mol\cdot m^{-2}\cdot s^{-1}$
N_0 = total number of time intervals measured at a given Reynolds number, 1
$q_w(t)$ = local instantaneous heat flux into or from a fluid element at the tube wall, $W\cdot m^{-2}$
$\bar{q}_w$ = local time-averaged heat flux at the interface, $W\cdot m^{-2}$
t = time, s
t^+ = dimensionless averaging time ($t^+=a\cdot(u^{*2}/\nu)$), 1
t_d = time at which the renewal process is detected, s
t_0 = characteristic age or mean age (Eq. 19), s
T^+ = dimensionless temperature {$T^+=[T_w-\bar{T}(y)]\rho c_p u^*/\bar{q}_w$}
T_b = temperature of the fluid bulk, K
T_f = film temperature [$T_f=(T_w+T_b)/2$], K
T^0 = dimensionless temperature in the wall region {$T^0=[T_w-\bar{T}(y)]/(T_w-T_b)$}, 1
T_w = temperature of the tube wall, K
$\bar{T}(y)$ = local time-averaged temperature, K
$T(y,t)$ = local instantaneous temperature in the wall region, K
u' = local axial velocity fluctuation ($u'=u-\bar{u}$), $m\cdot s^{-1}$
u_b = fluid velocity in the bulk, $m\cdot s^{-1}$
u_w = fluid velocity at the tube wall ($u_w=0$), $m\cdot s^{-1}$
$<u>$ = average value of the fluid velocity over the cross section of the tube, $m\cdot s^{-1}$
u^+ = dimensionless axial velocity [$u^+=\bar{u}(y)/u^*$], 1
$<u>^+$ = dimensionless average axial velocity ($<u>^+=<u>/u^*$), 1
u^0 = dimensionless axial velocity in the wall region [$u^0=\bar{u}(y)/u_b$], 1
u^* = friction velocity [$u^*=\sqrt{(\bar{\tau}_w/\rho)}$], $m\cdot s^{-1}$
$\hat{u}$ = conditionally averaged axial velocity, $m\cdot s^{-1}$
$\bar{u}(y)$ = local time-averaged axial velocity, $m\cdot s^{-1}$
$u(y,t)$ = local instantaneous axial velocity, $m\cdot s^{-1}$
U_∞ = free stream velocity, $m\cdot s^{-1}$
x = coordinate in the longitudinal direction, m
y = distance to the tube wall, m
y^+ = dimensionless distance to the wall ($y^+=yu^*/\nu$), 1
y^0 = dimensionless distance to the wall [$y^0=(y/d)Re(f/2)$]
z = dimensionless variable [$z=y/\{2\sqrt{(\nu t)}\}$], 1
z_0 = dimensionless variable [$z_0=y/\{2\sqrt{(\nu t_0)}\}$], 1

Greek letters

α = heat-transfer coefficient, $W\cdot m^{-2}\cdot K^{-1}$

β = transport property in Eqs. 9, 10, and 11
Γ = gamma function [$\Gamma(4/3) \approx 0.893$], 1
δ = boundary-layer thickness, m
δ_u = unreplenished fluid-layer thickness, m
Δc = concentration difference, $\text{mol} \cdot \text{m}^{-3}$
ΔT = temperature difference, K
$\Delta(\rho u)$ = momentum difference per unit of volume, $\text{kg} \cdot \text{m}^{-2} \cdot \text{s}^{-1}$
$\Delta\theta$ = small part of the time interval θ, s
ζ = dimensional physical quantity defined in Eq. 39
ζ_0 = dimensionless physical quantity defined in Eq. 51
η = dynamic viscosity, $\text{Pa} \cdot \text{s}$
η_b = dynamic viscosity evaluated at the bulk temperature, $\text{Pa} \cdot \text{s}$
η_w = dynamic viscosity evaluated at the wall temperature, $\text{Pa} \cdot \text{s}$
θ = age of a fluid element at the tube wall or time interval between two successive surface renewals, s
$\bar{\theta}$ = mean age of the fluid elements at the tube wall calculated with Eqs. 4 and 19, s
$\bar{\theta}_{\text{exp}}$ = measured value of $\bar{\theta}$, s
θ^+ = dimensionless parameter defined by $\theta^+ = u^* \sqrt{(\bar{\theta}_{\text{exp}}/\nu)}$, 1
κ = dimensionless physical quantity defined in Eq. 63
κ_0 = dimensionless physical quantity defined in Eq. 63
λ = thermal conductivity, $\text{W} \cdot \text{m}^{-1} \cdot \text{K}^{-1}$
ν = kinematic viscosity, $\text{m}^2 \cdot \text{s}^{-1}$
ξ = variable in Eq. 38, 1
π = 3.14159..., 1
ρ = density, $\text{kg} \cdot \text{m}^{-3}$
σ = surface tension, $\text{Pa} \cdot \text{m}$
$\tau_w(t)$ = local instantaneous shear stress exerted on the wall by a laminar flowing fluid element, Pa
$\bar{\tau}_w$ = local time-averaged wall-shear stress, Pa
$\varphi(\theta)$ = age distribution, s^{-1}

Dimensionless numbers

Fa = Fanning number ($Fa = k_m d/\nu$), 1
Fo = Fourier number for momentum transfer ($Fo = \nu t_0/d^2$), 1
Nu = Nusselt number ($Nu = \alpha d/\lambda$), 1
Pr = Prandtl number ($Pr = \nu/a$), 1
Re = Reynolds number ($Re = <u> d/\nu$), 1
Sc = Schmidt number ($Sc = \nu/D$), 1
Sh = Sherwood number ($Sh = kd/D$), 1

Literature Cited

Abramowitz, M., and I. A. Stegun, *Handbook of Mathematical Functions*, p. 297, 9th printing, Dover Publications, New York (1970).

Alfredsson, P. H., and A. V. Johansson, "Time Scales in Turbulent Channel Flow," *Phys. Fluids*, **27**, 1974 (1984).

Bakker, C. A. P., "Grensvlakstroming en Stofoverdracht Tussen Beweeglijke Fasen," PhD Thesis, Delft Univ. of Technology, The Netherlands (1965).

Batchelor, G. K., "Review of Momentum Transfer in Fluids," *J. Fluid Mech.*, **2**, 204 (1957).

Bird, R. B., W. E. Stewart, and E. N. Lightfoot, *Transport Phenomena*, p. 551, Wiley, New York (1960).

Blackwelder, R. F., and R. E. Kaplan, "On the Wall Structure of the Turbulent Boundary Layer," *J. Fluid Mech.*, **76**, 89 (1976).

Blasius, H., "Das Ahnlichkeitsgestetz bei Reibungsvorgängen in Flüssigkeiten," *Forsch. Ver. deut. Ing.*, **131** (1913).

Bogard, D. G., and W. G. Tiederman, "Burst Detection with Single Point Velocity Measurements," *J. Fluid Mech.*, **179**, 1 (1986).

Brodkey, R. S., K. N. McKelvey, and H. C. Hershey, "Mass Transfer at the Wall as a Result of Coherent Structures in a Turbulently Flowing Liquid," *Int. J. Heat Mass Transfer*, **21**, 593 (1978).

Brodkey, R. S., and H. C. Hershey, *Transport Phenomena—a Unified Approach*, 2nd printing, McGraw-Hill, New York (1989).

Cantwell, B. J., "Organized Motion in Turbulent Flow," *Ann. Rev. Fluid Mech.*, **13**, 1 (1981).

Chilton, T. H., and A. P. Colburn, "Mass Transfer (Absorption) Coefficients—Prediction from Data on Heat Transfer and Fluid Friction," *Ind. Eng. Chem.*, **26**, 1183 (1934).

Colburn, A. P., "A Method of Correlating Forced Convection Heat Transfer Data and a Comparison with Fluid Friction," *Trans. AIChE*, **29**, 174 (1933).

Corino, E. R., and R. S. Brodkey, "A Visual Investigation of the Wall Region in Turbulent Flow," *J. Fluid Mech.*, **37**, 1 (1969).

Danckwerts, P. V., "Significance of Liquid-Film Coefficients in Gas Absorption," *Ind. Eng. Chem.*, **43**(6), 1460 (1951).

Duduković, A., "Analogies Between Momentum, Heat and Mass Transfer in Dilute Polymer Solutions," *Encyclopedia of Fluid Mechanics*, Chap. 12, Vol. 7, N. P. Cheremisinoff, ed., Gulf Publishing, Houston (1988).

Eck, B., *Technische Strömungslehre*, p. 126, Springer-Verlag, New York (1973).

Einstein, H. A., and H. Li, "The Viscous Sublayer along a Smooth Boundary," *Trans. ASCE*, **82**, 293 (1956).

Fortuin, J. M. H., and P.-J. Klijn, "Drag Reduction and Random Surface Renewal in Turbulent Pipe Flow," *Chem. Eng. Sci.*, **37**, 611 (1982).

Friend, W. L., and A. B. Metzner, "Turbulent Heat Transfer Inside Tubes and the Analogy among Heat, Mass and Momentum Transfer," *AIChE J.*, **4**(4), 393 (1958).

Hanratty, T. J., "Turbulent Exchange of Mass and Momentum with a Boundary," *AIChE J.*, **2**(3), 359 (1956).

Harriott, P., "A Random Eddy Modification of the Penetration Theory," *Chem. Eng. Sci.*, **17**, 149 (1962).

Harriott, P., and R. M. Hamilton, "Solid-Liquid Mass Transfer in Turbulent Pipe Flow," *Chem. Eng. Sci.*, **20**, 1073 (1965).

Hart, J., "Single-Phase and Two-Phase Pipe Flow," PhD Thesis, Univ. of Amsterdam, The Netherlands (1988).

Higbie, R., "The Rate of Absorption of a Pure Gas into a Still Liquid during Short Periods of Exposure," *Trans. AIChE*, **31**, 365 (1935).

Hoogendoorn, C. J., *Fysische Transportverschijnselen II*, p. 169, Delftse Uitgevers Maatschappij b.v., Delft, The Netherlands (1985).

Johansson, A. V., and P. H. Alfredsson, "On the Structure of Turbulent Channel Flow," *J. Fluid Mech.*, **122**, 295 (1982).

Kim, H. T., S. J. Kline, and W. C. Reynolds, "The Production of Turbulence Near a Smooth Wall in a Turbulent Boundary Layer," *J. Fluid Mech.*, **50**, 133 (1971).

Kline, S. J., W. C. Reynolds, F. A. Schraub, and P. W. Runstadler, "The Structure of Turbulent Boundary Layers," *J. Fluid Mech.*, **30**, 741 (1967).

Linden, R. van der, "Transients in Turbulent Convective Heat Transfer to a Flow of Supercritical Helium," PhD Thesis, Delft Univ. of Technology, The Netherlands (1990).

Loughlin, K. F., M. A. Abul-Hamayel, and L. C. Thomas, "The Surface Rejuvenation Theory of Wall Turbulence for Momentum, Heat and Mass Transfer: Application to Moderate and High Schmidt (Prandtl) Numbers," *AIChE J.*, **31**(10), 1614 (1985).

Lu, S. S., and W. W. Willmarth, "Measurement of the Structure of the Reynolds Stress in a Turbulent Boundary Layer," *J. Fluid Mech.*, **60**, 481 (1973).

Luchick, T. S., and W. G. Tiederman, "Timescale and Structure of Ejections and Bursts in Turbulent Channel Flows," *J. Fluid Mech.*, **174**, 529 (1987).

Maanen, H. R. E. van, and J. M. H. Fortuin, "Experimental Determination of the Lump-Age Distribution in the Boundary Layer of a Turbulent Pipe Flow Using Laser-Doppler Anemometry," *Proc. Int. Symp. on Applications of Laser Techniques to Fluid Mech.*, Lisbon, Portugal (July 1982).

Maanen, H. R. E. van, and J. M. H. Fortuin, "Experimental Determination of the Random Lump-Age Distribution in the Boundary Layer of the Turbulent Pipe Flow Using Laser-Doppler Anemometry," *Chem. Eng. Sci.*, **38**, 399 (1983).

McAdams, W. H., *Heat Transmission*, 3rd ed., McGraw-Hill, New York (1954).

Meek, R. L., "The Periodic Viscous Sublayer in Turbulent Flow," *AIChE J.*, **16**(5), 841 (1970).

Meek, R. L., "Mean Period of Fluctuations Near the Wall in Turbulent Flows," *AIChE J.*, **18**, 854 (1972).

Mizushina, T., F. Ogino, Y. Oka, and H. Fukuda, "Turbulent Heat and Mass Transfer Between Wall and Fluid Streams of Large Prandtl and Schmidt Numbers," *Int. J. Heat Mass Transfer*, **14**, 1705 (1971).

Moens, F. P., "The Effect of Composition and Driving Force on the

Performance of Packed Distillation Columns: I and II," *Chem. Eng. Sci.*, **27**, 275 (1972).
Musschenga, E. E., P. J. Hamersma, and J. M. H. Fortuin, "Experimental Verification of the Random Surface Renewal Model for Turbulent Pipe Flow Using Laser-Doppler Anemometry," *Proc. Int. Symp. on Applications of Laser Techniques to Fluid Mech.*, Lisbon, Portugal, Paper 16.6 (July, 1990).
Musschenga, E. E., P. J. Hamersma, and J. M. H. Fortuin, "Drag Reduction and Random Surface Renewal in Turbulent Pipe Flow," *Proc. Int. Conf. on Laser Anemometry*, Cleveland, OH (Aug., 1991).
Narahari Rao, K., R. Narasimha, and M. A. Badri Narayanan, "The 'Bursting' Phenomenon in a Turbulent Boundary Layer," *J. Fluid Mech.*, **48**, 339 (1971).
Nijsing, R., "Predictions on Momentum, Heat, and Mass Transfer in Turbulent Channel Flow with the Aid of a Boundary Layer Growth-Breakdown Model," *Wärme- und Stoffübertragung*, **2**, 65 (1969).
Nikuradse, J., "Gesetzmäszigkeiten der Turbulenter Strömung in Glatten Rohren," *Forsch. Ver. deut. Ing.*, **356** (1932).
Perlmutter, D. D., "Surface-Renewal Models in Mass Transfer," *Chem. Eng. Sci.*, **16**, 287 (1961).
Perry, R. H., and D. Green, *Chemical Engineers' Handbook*, 6th ed., McGraw-Hill, New York (1984).
Pinczewski, W. V., and S. Sideman, "A Model for Mass (Heat) Transfer in Turbulent Tube Flow: Moderate and High Schmidt (Prandtl) Numbers," *Chem. Eng. Sci.*, **29**, 1969 (1974).
Ruckenstein, E., "A Note Concerning Turbulent Exchange of Heat or Mass with a Boundary," *Chem. Eng. Sci.*, **7**, 265 (1958).
Seidman, M. H., "Rough Wall Heat Transfer in a Compressible Turbulent Boundary Layer," AIAA, Paper No. 78 (1978).
Sherwood, T. K., R. L. Pigford, and C. R. Wilke, *Mass Transfer*, p. 5, McGraw-Hill, New York (1975).
Sideman, S., and W. V. Pinczewski, *Topics in Transport Phenomena*, Hemisphere, Washington (1975).
Sieder, E. N., and G. E. Tate, *Ind. Eng. Chem.*, **28**, 1429 (1936).
Strickland, J. H., and R. L. Simpson, "Bursting Frequencies Obtained from Wall Shear Stress Fluctuations in a Turbulent Boundary Layer," *Phys. of Fluids*, **18**, 306 (1975).
Toor, H. L., and J. M. Marchello, "Film-Penetration Model for Mass and Heat Transfer," *AIChE J.*, **4**, 97 (1958).
Thomas, L. C., P. J. Gingo, and B. T. F. Chung, "The Surface Rejuvenation Model for Turbulent Convective Transport—an Exact Solution," *Chem. Eng. Sci.*, **30**, 1239 (1975).
Thomas, L. C., "The Turbulent Burst Phenomenon: Inner Laws for u^+ and T^+," NATO Advanced Study Institute in Turbulence, Istanbul (1978).
Thomas, L. C., "The Surface Rejuvenation Model of Wall Turbulence: Inner Laws for u^+ and T^+," *Int. J. Heat Mass Transfer*, **23**, 1099 (1980).
Tiederman, W. G., "Eulerian Detection of Turbulent Bursts," Zoran P. Zarić Memorial International Symposium on Near-Wall Turbulence, Dubrovnik, Yugoslavia (May 16-20, 1988).
Wallace, J. M., H. Eckelmann, and R. S. Brodkey, "The Wall Region in Turbulent Shear Flow," *J. Fluid Mech.*, **54**, 39 (1972).
Weast, R. C., *Handbook of Chemistry and Physics*, A-95, No. 669, 61st ed., The Chemical Rubber Co., Cleveland, OH (1981).

Manuscript received July 2, 1991, and revision received Dec. 2, 1991.